UNIVERSIDADE DA BEIRA INTERIOR

Engenharia

4D Fuel Optimal Trajectory Generation from Waypoint Networks

Kawser Ahmed

Dissertação para obtenção do grau de mestre em

Engenharia Aeronáutica

(Ciclo de estudos integrado)

Orientador: Prof. Doutor Kouamana Bousson

Covilhã, fevereiro de 2016

Acknowledgements

I would like to express my sincere appreciation to Professor Kouamana Bousson for his support and guidance throughout this thesis and throughout my education at The University of Beira Interior. Finally, I would like to thank my family and friends for their support during my education at The University of Beira Interior.

Abstract

The purpose of this thesis is to develop a trajectory optimization algorithm that finds a fuel optimal trajectory from 4D waypoint networks, where the arrival time is specified for each waypoint in the network. Generating optimal aircraft trajectory that minimizes fuel burn and associated environmental emissions helps the aviation industry cope with increasing fuel costs and reduce aviation induced climate change, as CO_2 is directly related to the amount of fuel burned, therefore reduction in fuel burn implies a reduction in CO_2 emissions as well.

A single source shortest path algorithm is presented to generate the optimal aircraft trajectory that minimizes the total fuel burn between the initial and final waypoint in pre-defined 4D waypoint networks. In this work the 4D waypoint networks only consist of waypoints for climb, cruise and descent phases of the flight without the takeoff and landing approach. The fuel optimal trajectory is generated for three different lengths of flights (short, medium and long haul flight) for two different commercial aircraft considering no wind.

The Results about the presented applications show that by flying a fuel optimal trajectory, which was found by implying a single source shortest path algorithm (Dijkstra's algorithm) can lead to reduction of average fuel burn of international flights by 2.8% of the total trip fuel. By using the same algorithm in 4D waypoints networks it is also possible to generate an optimal trajectory that minimizes the flight time. By flying this trajectory average of 2.6% of total travel time can be saved, depends on the trip length and aircraft types.

Keywords

Fuel Conservation; Cost Index; Dijkstra's algorithm; 4D Waypoint navigation; Base of Aircraft Data (BADA);

Resumo

Esta tese tem como objetivo desenvolver um algoritmo de otimização de trajetória que permita encontrar uma trajetória de combustível ótima em uma redes de waypoint em 4D, onde o tempo de chegada é específico para cada waypoint da rede. Ao criar uma trajetória ótima que minimize o consumo de combustível da aeronare e as suas respetivas emissões poluentes, ajuda a indústria da aviação não só a lidar com o aumento nos custos dos combustíveis, bem como a reduzir a sua contribuição nas alterações climáticas, pois o CO_2 está diretamente relacionado com a quantidade de combustível queimado, logo uma redução no seu consumo implica que haja também uma redução nas emissões de CO_2.

O algoritmo “single source shortest path” é utilizado de forma a gerar uma trajetória ótima, que minimize o consumo de combustível entre o waypoint inicial e final de redes pré-definida de waypoint em 4D. Neste trabalho, esta redes consiste num conjunto de waypoints inseridos apenas nas fases de voo de subida, cruzeiro e descida, ignorando assim as fases de descolagem e aterragem. A trajetória de combustível ótima é criada para dois aviões comerciais diferentes em três distâncias de voo também diferentes (voo curto, médio e longo), sem considerar o vento.

Os resultados deste trabalho mostram que ao voar numa trajetória de combustível ótima, obtida através do algoritmo “single source shortest path” (Dijkstra’s algorithm), é possível reduzir o consumo total de combustível numa média de 2.8%, em voos internacionais. Utilizando o mesmo algoritmo numa rede de waypoints em 4D é também possível encontrar uma trajetória ótima que minimize o tempo de voo numa media de 2.6% do tempo total, consoante a distância da viagem e do tipo de aeronave.

Palavras-chave

Conservação de combustível; Cost Index; Dijkstra’s algorithm; Navegação por waypoints em 4D; Base of Aircraft Data (BADA);

Index

List of Figures ..xi
List of Tables xiii
List of Acronyms ..xv
List of Symbols xvii
1 Introduction 1
1.1 Motivation 1
1.2 Fuel Saving in Different Phases of Commercial Flight 3
1.2.1 Cruise Phase 4
1.2.2 Takeoff and Climb Phase 6
1.2.3 Descent and Approach Phase 7
1.3 Trajectory Optimization 9
1.4 Objectives 10
1.5 Outline 11
2 Dijkstra’s Algorithm 13
2.1 Pseudo-code of Dijkstra’s Algorithm 14
2.2 Representation of Graph 15
2.3 Implementation of Dijkstra’s in Flight Trajectory Optimization 16
3 Modeling of the 4D Waypoints Network 17
3.1 Navigation Model 18
3.2 Flight Constraints 18
3.3 Arrival Time of Each Waypoint 19
3.4 Engine Thrust 21
3.4.1 Maximum Climb and Take-off Thrust 21
3.4.2 Maximum Cruise Thrust 22
3.4.3 Descent Thrust 22
3.5 Fuel Consumption Model 23
3.5.1 Thrust Specific Fuel Consumption 23
3.5.2 Nominal Fuel Flow Rate 24
3.6 Consumed Fuel Between Waypoints 25
4 Optimal Trajectory Generation 27
4.1 Selection of Flights for Analysis 27
4.2 Selection of Aircraft for Analysis 28
4.3 Fuel Optimal Trajectory Generation 29
4.4 Time Optimal Trajectory Generation 29
4.5 Minimization of Delay of each Waypoint in Fuel and Time Optimal Trajectories. 30

4.5.1 Determination of coefficients 30
5 Simulation and Result 33
5.1 Short Haul Flight 33
5.1.1 Fuel Optimal Trajectory 35
5.1.2 Time Optimal Trajectory 36
5.2 Medium Haul Flight 37
5.2.1 Fuel Optimal Trajectory 38
5.2.2 Time Optimal Trajectory 39
5.3 Long Haul Flight 40
5.3.1 Fuel Optimal Trajectory 42
5.3.2 Time Optimal Trajectory 43
6 Conclusion and Discussions 45
6.1 Future work 46
7 References 47

List of Figures

Figure 1-1: Fuel Prices over the years in Dollar 1
Figure 1-2: Effect of the winglet on the vortex 2
Figure 1-3: Different phases of commercial flights from takeoff to landing. 4
Figure 1-4: Comparison of different cruise speeds 4
Figure 1-5: Optimum altitude determination at constant Mach number 5
Figure 1-6: Descent profile at given IAS 7
Figure 1-7: Typical descent phase of commercial flight 8
Figure 2-1: Pseudo-code for Dijkstra's algorithm 14
Figure 2-2: The execution of Dijkstra's algorithm 15
Figure 2-3: Representation of graph G into matrix 16
Figure 5-1: 3D fuel optimal trajectory in geocentric coordinates for short haul flight. 35
Figure 5-2: 3D time optimal trajectory in geocentric coordinates for short haul flight. 36
Figure 5-3: 3D fuel optimal trajectory in geocentric coordinates for medium haul flight. 39
Figure 5-4: 3D time optimal trajectory in geocentric coordinates for medium haul flight. 40
Figure 5-5: 3D fuel optimal trajectory in geocentric coordinates for long haul flight. 42
Figure 5-6: 3D fuel optimal trajectory in geocentric coordinates for long haul flight. 43

List of Tables

Table 1-1: ECON cruise Mach in different cruise wind conditions 5
Table 1-2: Impact of takeoff flap settings on fuel burn 6
Table 1-3: Fuel saving potential of two climb profile 7
Table 1-4: Fuel savings estimates for delayed flaps approach procedure 9
Table 4-1: Characteristics of airplane A1 and airplane A2 28
Table 5-1: List of waypoints in 1st trajectory of short haul flight 34
Table 5-2: List of waypoints in 2nd trajectory of short haul flight 34
Table 5-3: Total fuel consumed in different trajectories for short haul flight. 35
Table 5-4: Total time needed in different trajectories for short haul flight. 36
Table 5-5: List of waypoints in 1st trajectory of medium haul flight 37
Table 5-6:List of waypoints in 2nd trajectory of medium haul flight 38
Table 5-7: Total Fuel consumed in different trajectories for medium haul flight. 38
Table 5-8: Total time needed in different trajectories for medium haul flight. 39
Table 5-9: List of waypoints in 1st trajectory of long haul flight 41
Table 5-10: List of waypoints in 2nd trajectory of long haul flight 41
Table 5-11: Total Fuel consumed in different trajectories for long haul flight. 42
Table 5-12: Total time needed in different trajectories for long haul flight. 43

List of Acronyms

AGL	Above Ground Level
ATC	Air Traffic control
BADA	Base of Aircraft Data
CAEP	Committee on Aviation Environment Protection
CAS	Calibrated Air Speed
CDU	Control Display Unit
CI	Cost Index
FMC	Flight Management Computer
GHG	Green House Gas
GPS	Global Positioning System
GTF	Geared Turbofan Technique
IAS	Indicated Air Speed
ICAO	International Civil Aviation Organization
IPCC	Intergovernmental Panel on Climate Change
LRC	Long Range Cruise
MRC	Maximum Range Cruise
SID	Standard Instrument Departure
SR	Specific Range
STAR	Standard Terminal Arrival Route
TAS	True Air Speed
TOD	Top of Descent
TPBVPs	Two-Point Boundary Value Problems

List of Symbols

ε	Arrival time tolerance interval	
φ	Latitude	[deg]
γ	Flight path angle	[deg]
η	Thrust specific fuel consumption	[kg/(min.KN)]
λ	Longitude	[deg]
ρ	Air density	[kg/m^3]
τ	Arrival time at waypoint	[min]
ψ	Heading	[deg]
Δd	Distance between waypoints	[nm]
ΔT	Temperature deviation from standard atmosphere	[K]
a	Acceleration	[m/s]
a	Earth semi major axis	[nm]
C_L	Lift coefficient	
C_{f_1}, C_{f_2}	Thrust specific fuel consumption coefficient	
C_{f_3}, C_{f_4}	Descent fuel flow coefficient	
$C_{f_{cr}}$	Cruise fuel flow correction coefficient	
$C_{T_{c,1}}, C_{T_{c,2}}, C_{T_{c,3}}$	Climb thrust coefficient	
$C_{T_{c,4}}, C_{T_{c,5}}$	Thrust temperature coefficient	
$C_{T_{cr}}$	Maximum cruise thrust coefficient	
$C_{T_{des.app}}$	Approach thrust coefficient	
$C_{T_{des.\mathrm{high}}}$	High altitude descent thrust coefficient	
$C_{T_{des.\mathrm{ld}}}$	Landing thrust coefficient	
$C_{T_{des.\mathrm{low}}}$	Low altitude descent thrust coefficient	
D	Drag	
df	Consumed fuel between waypoints	[kg]
$d\tau$	Travel time between waypoints	[min]
E	Edges between vertices	
e	Eccentricity	
$f_{ap/ld}$	Approach and landing fuel flow rate	[kg/min]
f_{cr}	Cruise fuel flow rate	[kg/min]
$f_{\min}$	Minimum fuel flow rate	[kg/min]
f_{nom}	Nominal fuel flow rate	[kg/min]
G	Graph	
h	altitude	[feet]

H_p	Geo-potential pressure altitude	[feet]
$H_{p,des}$	Transition altitude	[feet]
M_d	Descent Mach number	[Mach]
P	Waypoint	
R_e	Earth radius	[nm]
S	Wing area	[m^2]
s	Source vertex	
Thr	Thrust	[KN]
$(Thr_{cruise})MAX$	Maximum cruise thrust	[KN]
$Thr_{des,\mathrm{app}}$	Approach thrust	[KN]
$Thr_{des,high}$	High altitude descent thrust	[KN]
$Thr_{des,\mathrm{ld}}$	Landing thrust	[KN]
$Thr_{des,\mathrm{low}}$	Low altitude descent thrust	[KN]
Thr_{maxclimb}	Maximum climb thrust	[KN]
$(Thr_{\mathrm{maxclimb}})ISA$	Maximum climb thrust at standard atmospheric condition	[KN]
V	Flight velocity	[Knots]
V	Vertices of the graph	
V_{CAS}	Calibrated air speed	[Knots]
V_{TAS}	True air speed	[Knots]
W	Aircraft Nominal weight	[kg]
w	Weight of the graph	
X,Y,Z	Geocentric Coordinates	[nm]

Chapter 1

1 Introduction

1.1 Motivation

Fuel saving on flight mission for commercial aircraft becomes an important factor nowadays in aviation mainly because of two reason, one is ever increasing fuel prices and other is to reduce the emission rates of greenhouse gases (GHG) into the atmosphere.

Improving aircraft operational efficiency has become a dominant theme in air transportation, as the airlines around the world have seen the price of fuel has risen sharply during the last decades (figure 1-1). The fuel cost represents around 30% of the operating costs for the airlines, thus the airlines are looking for different ways to reduce the flight operating costs by reducing the fuel consumption during the flight, also mounting scientific evidence of global climate change has spurred increased awareness of the importance of manmade greenhouse gas (GHG) emissions such as CO_2, resulting in significant pressure to reduce emissions. International civil aviation organization (ICAO) and committee on aviation Environmental protection (CAEP's) estimated that currently, aviation accounts for about 2% of total global CO_2 emissions and about 12% of the CO_2 from all transportation source [1], and by 2050, aviation's contribution could increase to 5% of the total human generated global warming. In terms of climate change, the Intergovernmental Panel on climate change (IPCC) estimated an increase in the earth's temperature of approximately 1.6 degrees Fahrenheit by 2050, of which about 0.09 degrees would be attributed to aviation. This increased fuel

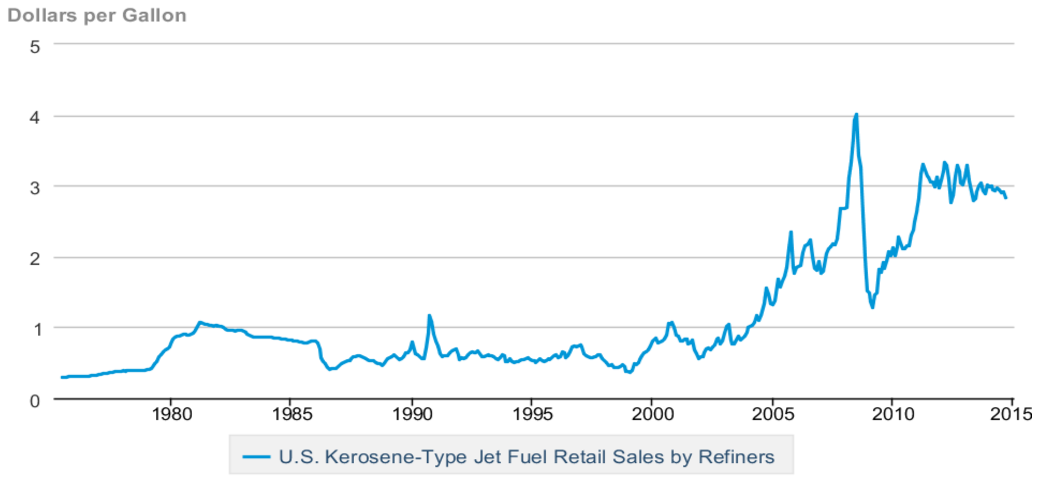

Figure 1-1: Fuel Prices over the years in Dollar

prices and environmental concerns have pushed airlines to reduce fuel consumption and to find margins for performance improvements [2].

Technological improvement such as development of more efficient engines, lighter materials, new aerodynamic designs, and the optimization of the flight trajectories can lead to reduction of fuel consumption. The engine builders propose new engine Pratt&Whitney, which developed the geared turbofan technique (GTF) which is endowed with speed reducer between the fan and the low pressure compressor, each component running at its optimal speed and improve the reactor performance, which results in reduction of fuel consumption. Currently Southwest airlines uses this engine for Airplane A1 series aircraft in order to increase engine efficiency and save fuel [3]. New aerodynamic design, such as winglets which reduce the aircraft drag by altering the airflow near the wingtip and decreases the vortex which makes it possible to reduce the fuel consumption (figure 1-2). The reduction of the fuel capacity at takeoff and weight reduction also helps to reduce the fuel consumption. Cathay Pacific airlines strip paint off some aircraft to reduce fuel burn. The polished silver fuselage makes the Boeing 747 about 200 kg lighter and saves more than HK$ 1.5 million on its annual fuel bill [4].

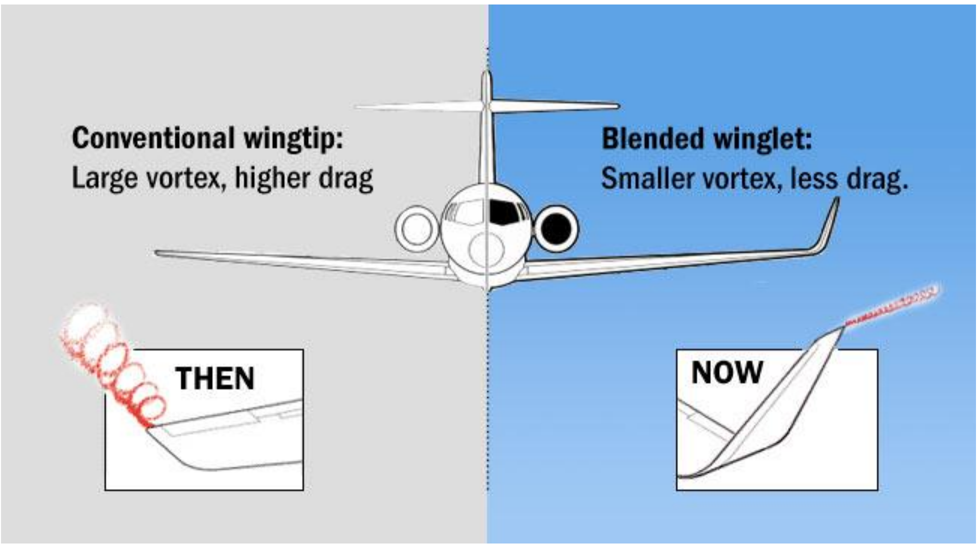

Figure 1-2: Effect of the winglet on the vortex

Efforts to modernize the aircraft fleet are limited by extremely slow and expensive process of new aircraft adoption, which can take decades, therefore it is important to find different alternatives to reduce the fuel consumption in current aircraft, which will likely to share the sky with most modern aircraft in near future. One of these alternatives is to optimize flight trajectories and traffic control procedure. Therefore, flight trajectory optimization with emphasis on fuel become really important to reduce the fuel consumption. The existing flight planning techniques are suboptimal. Hence, an fuel optimal flight path can significantly save fuel.

1.2 Fuel Saving in Different Phases of Commercial Flight

In commercial flight the rate of fuel burn mainly depends on ambient temperature, aircraft speed, and aircraft altitude. It also depend on aircraft weight which changes as fuel burned. The wind may provide a head or tail wind component which in turn will increase or decrease the fuel consumption by increasing or decreasing the air distance to be flown.

A practical solution that reduces the cost associated with time and fuel consumption during flight is the cost index (CI). The value of the CI reflects the relative effects of fuel cost on overall trip cost as compared to time-related direct operating cost. The cost index (CI) is shown in (equation 1.1).

$$CI = \frac{TimeCost \sim (€ / hr)}{FuelCost \sim (€ / kg)} \tag{1.1}$$

The flight crew enters the company calculated CI into the control display unit (CDU) of the flight management computer (FMC). The FMC uses this number and other performance parameters to calculate economy climb, cruise and descent speeds.

For all the aircraft models, the minimum value of cost index equal to zero results in maximum range airspeed and minimum trip fuel, but this configuration ignores the time cost. In the case when the cost index is maximum, the flight time is minimum, the velocity and the Mach number are maximum, but ignores the fuel cost.

The time related cost in CI depend on various things, such as flight crew wages, that can have an hourly cost associated with them, engines, auxiliary power units, and the airplanes can be leased by the hour and the maintenance can be accounted by the hour. As a result each of these items may have a high direct time costs, in such case CI is large to minimize the time. In the case where most costs are fixed, the CI is very low to minimize the fuel cost. The cost index allows finding a compromise between the fuel burn and the time according to the costs of both, to reduce the flight cost [5].

Commercial flights follow the following phases: Take-off, climb, cruise, descent and approach. Each of these phases may be divided into several flight segments. Mathematically each flight segment can be described by two constant control variables selected from among engine thrust settings, Mach number or calibrated airspeed, and altitude rate or flight path angle. Different phases of flight are shown in (figure 1-3). The following subsections provide more details about fuel saving on different phases of flight.

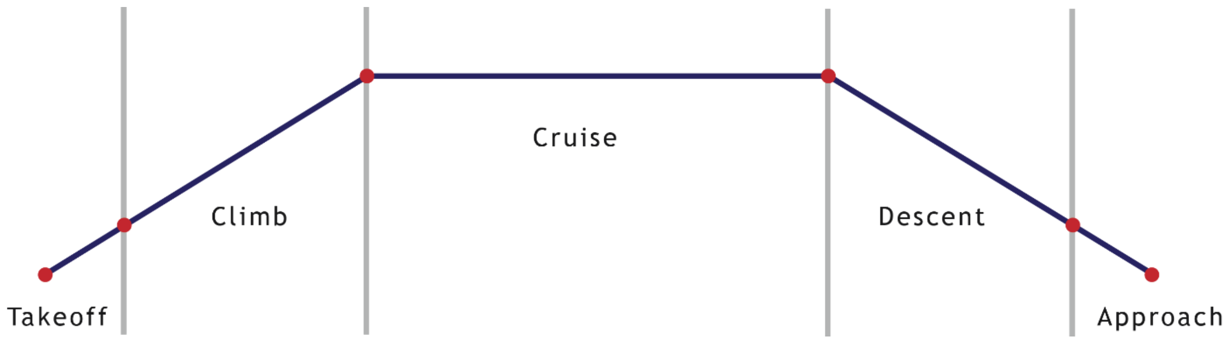

Figure 1-3: Different phases of commercial flights from takeoff to landing.

1.2.1 Cruise Phase

In general except for short flight trajectory, the largest percentage of the trip time and the trip fuel are consumed typically in cruise phase of flight, hence it is really important to have the best cruise condition to reduce the fuel consumption. The two variables which affect the travel time and the fuel burn most, are the cruise speed, and the altitude or flight level. The correct selection of the cruise parameters is therefore fundamental in minimizing fuel or operating cost, study shows that aircraft consume less fuel when flown slower or when flown higher. However there are limits to these laws. Flying slower than the maximum range speed will increase the block fuel, as will flying higher than an optimum altitude.

There are two theoretical speed selections for cruise phase of flight. The traditional speed is long range cruise (LRC), which is the speed that will provide the furthest distance traveled for a given amount of fuel burned and maximum range cruise (MRC) is the minimum fuel burned for a given cruise distance. Since fuel is not the only direct cost associated with a flight, a further refinement in the speed for most economical operation is ECON speed, based on entered CI. Which include some tradeoffs between trip time and trip fuel. The LRC speed is almost universally higher than the speed that will result from using CI selected by most carriers. But the MRC speed has the better fuel mileage

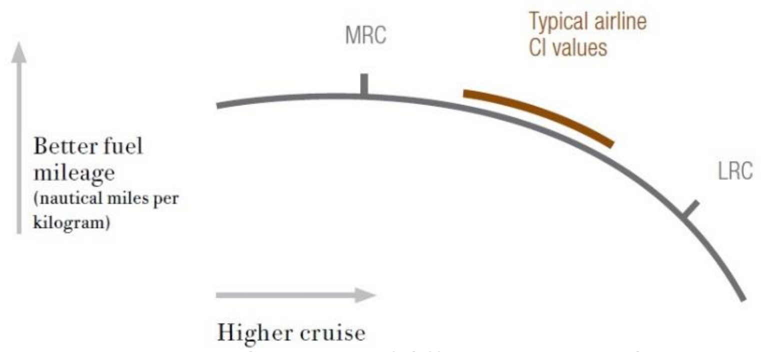

Figure 1-4: Comparison of different cruise speeds

for all the cruise speed (figure 1-4). So the best strategy to conserve fuel is to select the MRC speed, which has CI value equal to zero.

The specific range (SR) changes with the altitude at a constant Mach number, it is apparent that, for each weight, there is an altitude where SR is maximum. This altitude is referred to as " optimum altitude" (figure 1-5). The optimum altitude is not constant and changes over the period of a long flight as atmospheric condition and the weight of the aircraft changes. A large change in temperature will significantly alter the optimum altitude with a decrease in temperature corresponding to an increase in altitude.

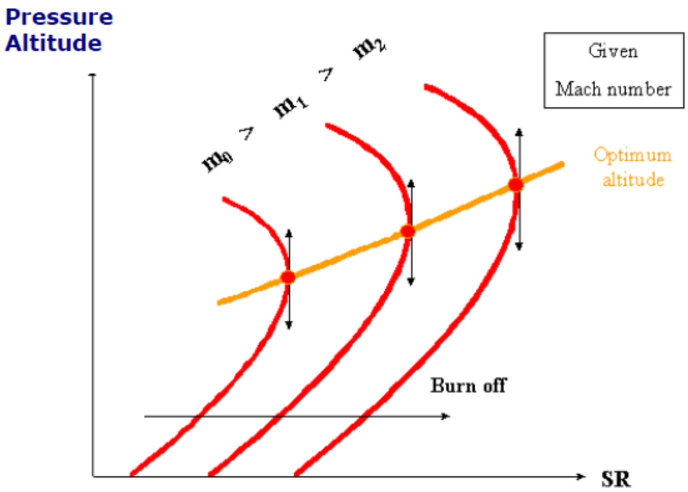

Figure 1-5: Optimum altitude determination at constant Mach number

When the aircraft flies at the optimum altitude, it is operated at the maximum lift to drag ratio corresponding to the selected Mach number. The maximum range cruise (MRC) Mach number gives the best specific range. Nevertheless, for practical operation, a long range cruise (LRC) Mach number procedure gains a significant increase in speed compare to MRC with only a 1% loss in specific range. Like the MRC, the LRC speed also decreases with decreasing weight, at constant altitude [6]

The LRC and the MRC speed calculated by the FMC is typically not adjusted for winds at cruise altitude. They are ideal only for Zero wind conditions. While the ECON speed is optimized for all cruise wind conditions (table 1-1). For example, in the presence of strong tailwind, the ECON speed will be reduced in order to maximize the advantage gained from the tailwind during cruise. Conversely, the ECON speed will be increased when flying into a head wind in cruise to minimize the penalty associated with the head wind [7].

Table 1-1: ECON cruise Mach in different cruise wind conditions

Cost Index	100 Kt Tailwind	Zero wind	100 Kt Headwind
0	0.773	0.773	0.785
80	0.787	0.796	0.803
MAX	0.811	0.811	0.811

1.2.2 Takeoff and Climb Phase

A standard instrument departure (SID) procedure or a departure procedure which defines a pathway from an airport runway to a waypoint on an airways, so that an aircraft can join the airway system in a controlled manner.

The climb phase has some restrictions. Upper and lower bound of flight path angle γ is primarily maintained because of passenger comfort and are also in effect throughout an entire flight. Another restriction imposed on the entire flight limits calibrated airspeed (V_{CAS}) 250 knots or less below altitude of 10,000 feet (3,048 m).

An important consideration when seeking fuel saving in the takeoff and climb phase of flight is the takeoff flap settings. The lower the flap setting, the lower the drag, resulting less fuel burned. (table 1-2) Shows the effect of takeoff flap setting on fuel burn from break release to a pressure altitude of 10,000 feet (3,048 m), assuming an acceleration altitude of 3,000 feet (914 m) above ground level (AGL).

Table 1-2: Impact of takeoff flap settings on fuel burn

Airplane Model	Takeoff Flap settings	Takeoff Gross weight (kg)	Fuel used (kg)	Fuel Differential (kg)
	5		578	-
737-800 Winglets	10	72,575	586	8
	15		588	10
747-400	10	328,855	2,555	-
	20		2,618	63

Another area in the takeoff and climb phase where fuel burn can be reduced is in the climb out and cleanup operation. If the flight crew performs acceleration and flap retraction at a lower altitude than the typical 3,000 feet (914 m), the fuel burn is reduced because of the drag is being reduced earlier in the climb out phase.

(table 1-3) Shows two standard climb profile for both airplanes. Profile 1 is a climb profile with acceleration and flap retraction beginning at 3,000 feet (914 m) above ground level (AGL), Profile 2 is a climb profile with acceleration to flap retraction speed beginning at 1,000 feet (305 m) AGL. Generally when airplanes fly profile 2 they use 3 to 4 percent less fuel than profile 1 [8].

Table 1-3: Fuel saving potential of two climb profile

Airplane model	Takeoff Gross weight (kg)	Profile type	Takeoff Flap setting	Fuel used (kg)	Fuel Differential (kg)
737-800 Winglets	72,575	1	10	2,374	-
		2		2,307	67
747-400	328,855	1	10	9,549	-
		2		9,313	236

1.2.3 Descent and Approach Phase

There are two main parameters to act on when willing to lower the fuel burn for the descent phase: the speed and the descent gradient whose combination determines the thrust required. The normal procedure for a descent is to select 3º descent slope and to maintain the Indicated air speed (IAS) by adjusting the thrust.

Descending at a higher slope enables to save fuel, as less thrust is required for the descent. The top of descent (TOD) occurs later and the flight at cruise level is longer. Beside, at a given gradient of descent, the slower the IAS selected, the less fuel is burnt during the descent, as less thrust is required (figure 1-6).

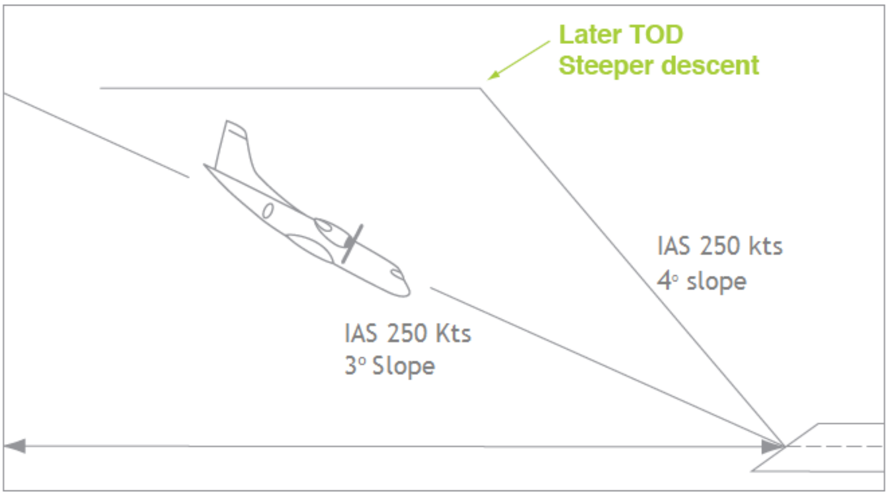

Figure 1-6: Descent profile at given IAS

Most of the airlines follow standard terminal arrival route (STAR) or an arrival procedure which defines a pathway from a waypoint on an airway to an airport runway, so that aircraft can leave the airway system in a controlled manner. STAR usually covers the phase of the flight that lies between top of descent from cruise and the final approach to a runway for landing.

The entire descent is considered to use idle thrust, but in practice a varying throttle will generally be required. As the cruise phase ends, the aircraft enters a constant altitude deceleration until it reaches its specified descent Mach number M_d, which is less than the cruise Mach. This transitions into a constant Mach descent segment and is followed by a constant Calibrated Airspeed V_{CAS} segment as the aircraft descends. At approximately 10,000 feet the aircraft enters a constant altitude or shallow descent segment until it decelerates to a Calibrated Airspeed V_{CAS} of 250 knots as is required under 10,000 feet. The aircraft then maintains a Calibrated Airspeed V_{CAS} of under 250 knots until it descends to approximately 3,000 feet where it begins the final landing Approach (figure 1-7).

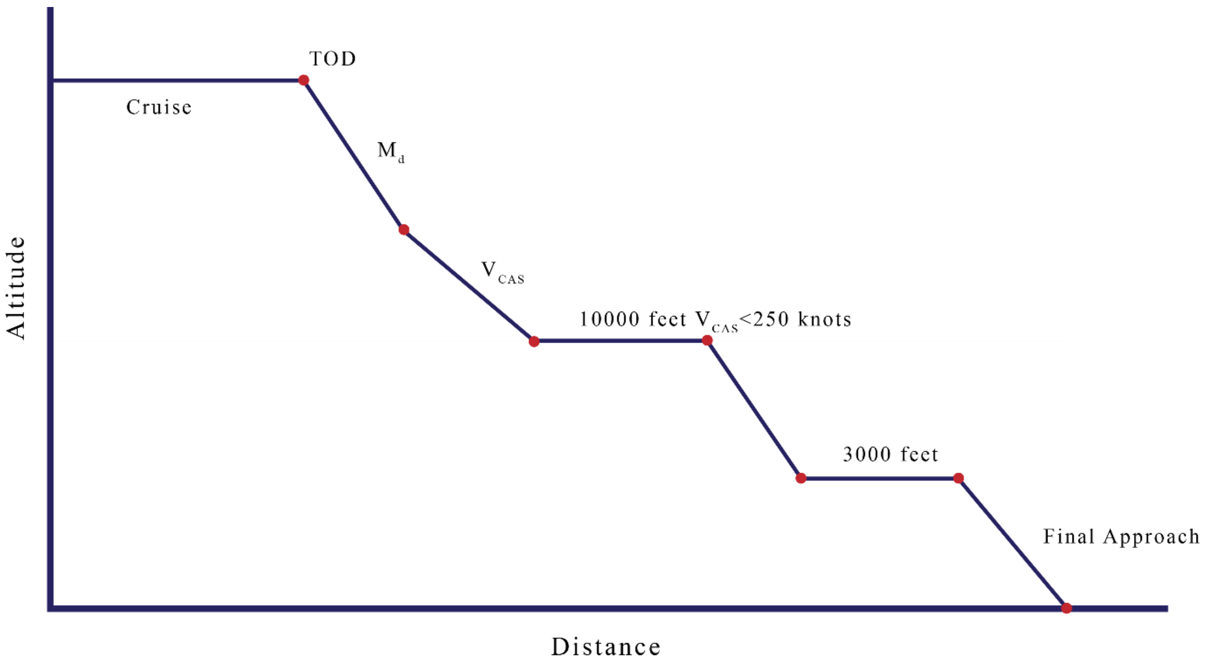

Figure 1-7: Typical descent phase of commercial flight

Low-drag delayed flaps or noise abatement approach is another type of descent approach. This approach is flown in a low drag configuration at a speed considerably higher than the final approach speed. At the appropriate time, power is reduced to idle and the flaps and gear are extended while decelerating to final approach speed. The throttles are partially advanced to initiate engine acceleration prior to selecting final approach flaps and are further advanced to normal approach power as the final approach speed is reached. The configuration and power changes are scheduled so as to stabilize in the landing configuration at a target altitude above 152 m (500 feet), selected by the pilot. The remainder of the approach is conventional [9].

Depending on the flap settings and airplane model, the delayed flaps approach uses 7 to 173 fewer kilograms of fuel than the standard approach with the same flap settings (table 1-3). Flight crews can vary their approach procedures and flap selections to match the flight's strategic objectives, which almost always include fuel conservation, noise abatement, and emissions reduction [10].

Table 1-4: Fuel savings estimates for delayed flaps approach procedure

Airplane Engine	Landing weight (kg)	Landing Flap (deg)	Procedure	Fuel Burned (kg)	Fuel differential (kg)
737-800 CFM56-7B24	54,431	30	Standard	104	-
			Delayed	97	7
		40	Standard	121	-
			Delayed	104	17
747-400 CF6-80C2B1F	204,116	25	Standard	268	-
			Delayed	245	23
		30	Standard	277	-
			Delayed	104	173

1.3 Trajectory Optimization

Classical aircraft trajectory optimizations are solved by applying calculus of variations to determine the optimality conditions, requiring the solution of non-linear two-point boundary value problems (TPBVPs) [11]. Alternatively, a more general solution to aircraft trajectory optimization can be obtained by singular perturbation theory which approximates solutions of high order problems by the solution of a series of lower order systems with the system dynamics separated into low and fast modes [12], [13].

With the tremendous advancement in numerical computing power, TPBVPs can be converted to nonlinear programming problems that are solvable even for problems with many variables and constraints using numerical algorithms such as direct collocation methods. Neglecting aircraft dynamics and applying shortest path algorithms in graph theory, an optimal trajectory can be approximated by the path that minimizes the total link cost connecting the origin and destination in a pre-defined network. The graph methods often require large computation time and memory space but guarantee global optimal solutions. In this thesis the single source shortest path algorithm was used to generate the fuel optimal trajectory.

This study is restricted to the climb, cruise and descent phases of the flight and ignores the takeoff and landing approach, and assuming the initial and final waypoints are at altitude of 3000 feet, where in the initial waypoint the aircraft begins the climb phase and in the final waypoint the aircraft begins the landing approach.

1.4 Objectives

The objective of this thesis is to find an optimal trajectory in 4D waypoint networks by using a single source shortest path algorithm (Dijkstra's algorithm) which minimizes the fuel burn. The objective can be fulfilled by achieving the following three goals:

1. To select a network of waypoints in 3D $P_k = (\lambda_k, \varphi_k, h_k)^T$ between initial and final waypoints, then calculating the associated arrival time τ_k in each waypoint.
2. To establish a method to calculate the associated consumed fuel df_k between the waypoints in the network using Base of Aircraft Data (BADA) .
3. Implementation of the Dijkstra's shortest path algorithm to find out the fuel optimal trajectory in 4D waypoint network between the initial and final waypoint.

This work primarily attempts to quantify benefits of fuel optimal trajectory which was found by implying the Dijkstra's shortest path algorithm. In this work, a benefit is meant to imply a reduction in fuel burn due to using the Dijkstra's shortest path algorithm to the actual unimproved flight.

As CO_2 is directly related to the amount of fuel burned, reduction in fuel consumption implies a reduction in CO_2 emissions as well. Therefore this analysis answers the question: How much can fuel burn and CO_2 emission be reduced in flight if aircraft are operated in fuel optimal trajectory? This work also attempts to quantify the benefits of time optimal trajectory which reduces the total travel time of the trajectory.

Optimal trajectories were generated for three different lengths of flight, they are short haul flight (Lisbon – Geneva), medium haul flight (Lisbon – Stockholm) and long haul flight (Lisbon – Montreal). In this work the trajectories are in climb, cruise and descent phases of the flight, considering no wind.

The key aspect of this thesis is a detailed comparison between actual flight trajectories and corresponding more efficient trajectories, thus giving the most realistic estimate of improvement potential.

1.5 Outline

The thesis is organized as follows, with major contribution of each chapter highlighted:

- Chapter 1 describes the motivation of the work and the state of art about fuel saving in flight trajectory.
- Chapter 2 described the Dijkstra's shortest path algorithm and convert a waypoint network graph into a matrix.
- Chapter 3 briefly describes the modeling of waypoint network by calculating the associated travel time and consumed fuel between the waypoints.
- Chapter 4 describes the fuel and time optimal trajectory generation by using Dijkstra's algorithm and minimization of delay of each waypoint in these trajectories.
- Chapter 5 presents the simulation results for the fuel and time optimal trajectory and compare the results with different trajectories.
- Chapter 6 gives a summary of the work, provides conclusions, discussions, and present a future work recommendations.

Chapter 2

2 Dijkstra’s Algorithm

Dijkstra’s algorithm is a simple greedy algorithm to solve single source shortest paths problem, it was conceived by a Dutch computer scientist Edsger Dijkstra in 1956 and was first published in 1959. The algorithm exists in many variants; Dijkstra's original variant finds the shortest path between two vertices, but a more common variant fixes a single vertex as the "source" vertex and finds shortest paths from the source to all other vertices in the graph, producing a shortest-path tree.

Dijkstra’s algorithm uses the greedy approach to solve the single source shortest path problem. It can also be used for finding costs of shortest paths from a single source vertex to a single destination vertex by stopping the algorithm once the shortest path to the destination vertex has been determined. For example, if the vertices of the graph represent cities and edge path costs represent driving distances between pairs of cities connected by a direct road, Dijkstra’s algorithm can be used to find the shortest route between one city and all other cities.

Dijkstra’s Algorithm is the most common single-source shortest path algorithm. It require three inputs (G, w, s) they are the graph G, the weights w, and the source vertex s. Graphs are often used to model networks in which one travels from one point to another. A graph G (V, E) refers to a collection of vertices V and a collection of edges E that connect pairs of vertices and assuming all edge costs are non-negative, thus there are no negative cycles and shortest paths exists for all vertices reachable from source vertex s. As a result, a basic algorithm problem is to determine the shortest path between vertices in a graph.

Graphs G (V, E) are simple to define, the waypoints are the vertices V and there is edge E between two waypoints, in the case of fuel optimal trajectory, the consumed fuel df_k from one waypoint to another is the edge of these waypoints or vertices, and in the case of time optimal trajectory, the travel time $d\tau_k$ from one waypoint to another is the edge of these waypoints (vertices). In both cases initial waypoint is the source vertex and the final waypoint is the destination vertex.

2.1 Pseudo-code of Dijkstra's Algorithm

To find the shortest path or to find the path with lowest cost between the source and destination vertices, the Dijkstra's algorithm must first initialize its three important arrays. First, the array S contains the vertices that have already been examined or relaxed. It first starts as the empty set, but as the algorithm progresses, it will fill with each vertex until all are examined. Then, the distance array d[x] is defined to be an array of the shortest paths from source s to x. Finally, Q is simply the data type used to form the list of all the vertices . In this case, it is a priority queue.

Now the algorithm moves into the shortest path calculation. The function will have to run as long as it takes to relax each edge for each vertex. Next, the algorithm uses "ExtractMin" to extract a vertex u from Q, this vertex u corresponding to the smallest shortest path estimate of any vertex in Q, and then adds it to set S (The first time though this loop, u = s). Then the algorithm compare every edge that connects to this newly chosen vertex u. If the adjacent vertex v currently has a distance to the source that is greater than the distance to u plus the distance between u and v, then the algorithm update the distance to v. After completion of this step, we now have an array d[x] that holds the value for the shortest distance from the source to each of the vertices in the graph. The pseudo-code for Dijkstra's algorithm is shown in (Figure 2-1).

$dijkstra\ (G, w, s)$

$d[s] = 0$
$for\ each\ v \in V - \{s\}$
    $do\ d[v] = \infty$
$S = \emptyset$
$Q = V$

$while\ Q \neq \emptyset$
    $do\ u = ExtractMin(Q)$
    $S = S \cup \{u\}$
    $for\ each\ v \in adj\ \{u\}$
        $do\ if\ d[v] > d[u] + w(u, v)$
            $then\ d[v] = d[u] + w(u, v)$

end

Figure 2-1: Pseudo-code for Dijkstra's algorithm

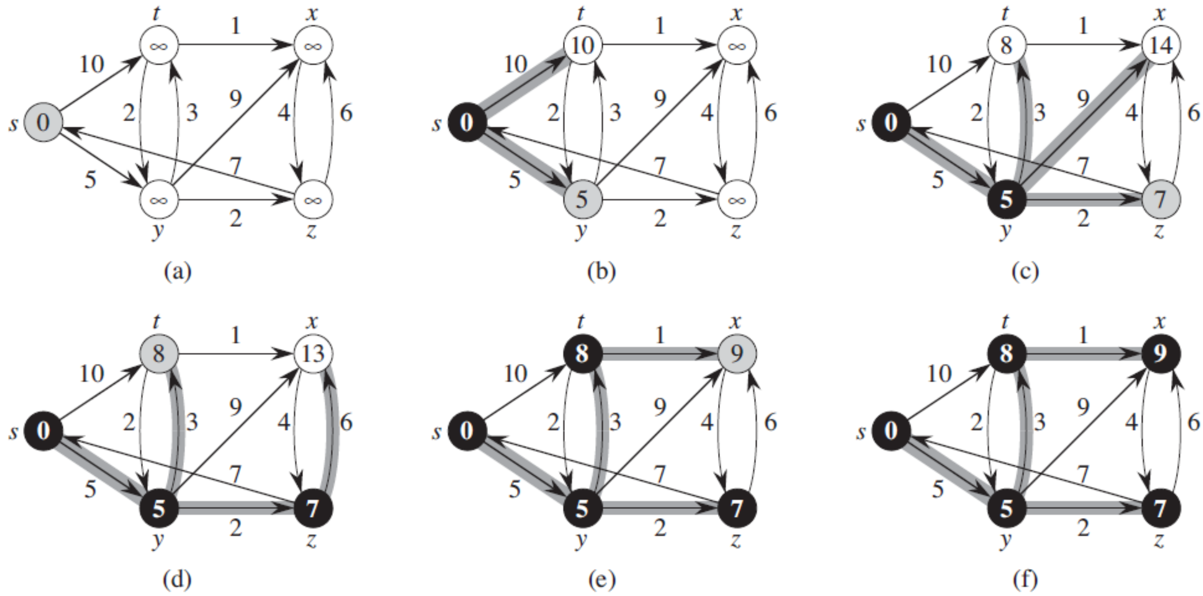

Figure 2-2: The execution of Dijkstra's algorithm

In (figure 2-2) a full example of the Dijkstra's algorithm operation is shown. The source s is the leftmost vertex. The shortest path estimates appears within the vertices, and shaded edges indicate predecessor values. Black vertices are in the set S, and the white vertices are in the min-priority Q. (a) The situation just before the first iteration of the while loop. The shaded vertex has the minimum d value and is chosen as vertex u. (b) – (f) The situation after each successive iteration of the while loop. The d value and predecessors shown in part (f) are the final values [14] [15] [16].

2.2 Representation of Graph

In order to input data into mathematics software in this case "Matlab", it is important to have some sort of method in which to describe the graph. One way to input the graph G into Matlab is in the form of a square matrix. The matrix will always be of $(n \times n)$ dimension where n is equal to the number of vertices in the graph. Each row will represent the vertex from which we are traveling. Each column will represent the vertex to which we are traveling to.

The matrix G is a representation of the graph with three vertices. Vertex A corresponds to row and column 1, B to row and column 2, etc. Matrix G shown below is the matrix representation of the graph (figure 2-3).

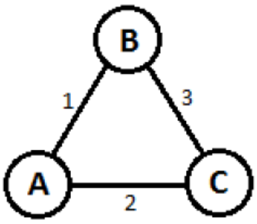

$$G = \begin{bmatrix} 0 & 1 & 2 \\ 1 & 0 & 3 \\ 2 & 3 & 0 \end{bmatrix}$$

Figure 2-3: Representation of graph G into matrix

It can now be seen that the cost from A to B will correspond to row 1, column 2 in the matrix. Therefore, G [1, 2] is equal to 1, G [1, 3] is equal to 2, and G [2, 3] is equal to 3. Also all of the elements in the diagonal of the matrix are equal to 0. This is a result of describing the cost from one vertex to itself, which is clearly zero. Also, the matrix should be symmetric across the diagonal. The matrix being symmetric would imply $w\ (x,\ y) = w\ (y,\ x)\ when\ \forall x,\ y \in G$.

2.3 Implementation of Dijkstra’s in Flight Trajectory Optimization

In addition to the basic formulation of the Dijkstra’s algorithm, the following aspects must be defined specifically for the flight trajectory optimization problem. The number of vertices (waypoints) from initial to final waypoints, the edge (consumed fuel or travel time) between the vertices, defining the source and destination vertices (waypoints). Once the above aspects have been accurately defined, Dijkstra’s algorithm will determine the shortest path using the method described previously.

Chapter 3

3 Modeling of the 4D Waypoints Network

Waypoints are sets of coordinates that identify a point in physical space. It normally defined by longitude λ, latitude φ, and altitude h. For 4D waypoint navigation it also defined by the arrival time τ at that waypoint P.

Waypoints have only become widespread for navigational use by the layman since the development of advanced navigational system, such as Global Positioning System (GPS) and certain other type of radio navigation.

In the modern world, waypoints are increasingly abstract, often having no obvious relationship to any distinctive features of the real world. These waypoints are used to help define invisible routing paths for navigation. For example artificial airways created specifically for purpose of air navigation, often have no clear connection to features of the real world, and consists only of a series of abstract waypoint in the sky through which pilots navigates, these airways are designed to facilitate air traffic control and routing of traffic between heavily traveled locations.

Suppose the waypoints network consists of N sets of waypoints, where P_1 is the initial waypoint and P_N is the final waypoint. Each waypoint P_k, (k =1,2,…., N) is defined by the geodetic coordinates $\lambda_k, \varphi_k, h_k$, by considering the arrival time in each waypoint τ_k, the waypoint P_k can be described as a four-dimensional state vector:

$$P_k = (\lambda_k, \varphi_k, h_k, \tau_k)^T \tag{3.1}$$

Where, λ_k and φ_k are the longitude and latitude of waypoint P_k, h_k is the altitude (with respect to sea level). The following subsections represent the navigation model and constraints of 4D waypoints network [17].

3.1 Navigation Model

The following differential equations model the dynamics of the navigation process:

$$\dot{\lambda} = \frac{V\cos\gamma\sin\psi}{(R_e + h)\cos\varphi} \tag{3.2}$$

$$\dot{\varphi} = \frac{V\cos\gamma\cos\psi}{(R_e + h)} \tag{3.3}$$

$$\dot{h} = V\sin\gamma \tag{3.4}$$

$$\dot{V} = u_1 \tag{3.5}$$

$$\dot{\gamma} = u_2 \tag{3.6}$$

$$\dot{\psi} = u_3 \tag{3.7}$$

Where, V = flight velocity, γ = flight path angle, ψ =heading (with respect to the geographical north), λ = longitude, φ = latitude, h = the altitude (with respect to sea level), R_e is the Earth radius. The variables u_1 , u_2 , and u_3 are respectively the acceleration, the flight path angle rate and the heading rate. The state vector x and control vector u of the above model are described respectively as:

$$x = (\lambda, \varphi, h, V, \gamma, \psi)^T$$

$$u = (u_1, u_2, u_3)^T$$

3.2 Flight Constraints

The real world flight operate under several constraints, due to aircraft performance, aerodynamic structural limits, safety reasons, the mission and other factor.

Velocity, V :

$$V_{\min} \le V \le V_{\max} \tag{3.8}$$

Acceleration, $a = \dot{V}$:

$$a_{\min} \le a \le a_{\max} \tag{3.9}$$

Flight path, γ :

$$\gamma_{\min} \le \gamma \le \gamma_{\max} \tag{3.10}$$

Flight path angle rate, $\dot{\gamma}$:

$$\dot{\gamma}_{\min} \le \dot{\gamma} \le \dot{\gamma}_{\max} \tag{3.11}$$

Heading rate, $\dot{\psi}$:

$$\dot{\psi}_{\min} \le \dot{\psi} \le \dot{\psi}_{\max} \tag{3.12}$$

3.3 Arrival Time of Each Waypoint

The 4D navigation consists of traveling through a sequence of predefined point in a given time of flight, which in turn define the trajectory of the flight. Assuming that the waypoint P_k is already defined by the geodetic coordinates longitude λ_k , latitude φ_k , and altitude h_k , where the scheduled time of arrival τ_k at this waypoint is unknown. To compute this unknown arrival time of each waypoint P_k , the distance between this waypoint P_k and its previous waypoint P_{k-1} from where the aircraft is arriving and the average velocity of the aircraft between this two waypoints are required.

The trajectory generation requires a geocentric coordinates system. To calculate the distance between two waypoints, the 3D waypoint need to be transformed from usual geodetic coordinates system to geocentric coordinates system. The 3D waypoint P_k is defined by the following way:

$$P_k = (\lambda_k, \varphi_k, h_k)^T \tag{3.13}$$

Now to transform these geodetic coordinates to geocentric coordinates, the following equation need to be applied [18].

$$X_k = (N_k + h_k)\cos\varphi_k \cos\lambda_k \tag{3.14}$$

$$Y_k = (N_k + h_k)\cos\varphi_k \sin\lambda_k \tag{3.15}$$

$$Z_k = [N_k(1-e^2)+h_k]\sin\varphi_k \tag{3.16}$$

Being a is the Earth semi major axis and e its eccentricity, N_k can be calculated as follows:

$$N_k = \frac{\mathrm{a}}{\sqrt{1-e^2\sin^2\varphi_k}} \tag{3.17}$$

After transforming the 3D waypoint from geodetic coordinates into geocentric coordinates system, now it is possible to calculate Δd_k (the distance between two waypoints P_{k-1} to P_k) by using the following equation:

$$\Delta d_k = \sqrt{(\mathrm{X}_k - X_{k-1})^2 + (\mathrm{Y}_k - Y_{k-1})^2 + (\mathrm{Z}_k - Z_{k-1})^2} \tag{3.18}$$

To estimate the appropriate velocity of the aircraft V_k at any waypoint P_k, the following equation can be used:

$$V_k = \sqrt{\frac{2W}{\rho_k C_L S}} \tag{3.19}$$

Where, W is the aircraft nominal weight, C_L is the lift coefficient, S is the wing area of the aircraft and ρ_k is the air density (varies with altitude) at waypoint P_k. It is possible to get the appropriate velocity at any waypoint P_k from Base of Aircraft Data (BADA), where true air speed, V_{TAS} [kt] is specified for different aircraft for different flight level and phases of the flights [19].

By using the distance between two waypoints and the velocity of the aircraft in both waypoints the arrival time of each waypoint can be computed as follow:

$$d\tau_k = \frac{\Delta d_k}{\frac{V_k + V_{k-1}}{2}} \tag{3.20}$$

Where, $d\tau_k$ is the time needed to go from waypoint P_{k-1} to P_k. So the arrival time of waypoint P_k from the initial waypoint can be described as follow:

$$\tau_k = \tau_{k-1} + d\tau_k \tag{3.21}$$

In practice, the aircraft may not pass through the waypoint P_k exactly at this specified time τ_k due to disturbances. Therefore, an appropriate way is rather imposing a time tolerance ε in (equation 3.21).

$$\tau_k = \tau_{k-1} + \varepsilon \times d\tau_k \qquad (3.22)$$

Where, ε is the tolerance time interval for arrival at a determined waypoint [$1.0 \le \varepsilon \le 1.4$], if the altitude of waypoints P_{k-1} and P_k are same, then the tolerance ε can be assumed 1.

3.4 Engine Thrust

To calculate the nominal fuel flow rate, it is necessary to calculate the engine thrust at different phases of flight. The BADA model provides coefficients that allow the calculation of the following thrust levels:

- Maximum climb and take-off,
- Maximum cruise,
- Descent.

3.4.1 Maximum Climb and Take-off Thrust

The maximum climb thrust at standard atmosphere conditions, $(Thr_{\text{maxclimb}})\text{ISA}$, is calculated as a function of geo-potential pressure altitude, H_p [ft]; true airspeed, V_{TAS} [kt]; and temperature deviation from standard atmosphere, ΔT [K]. Here only jet engine type was considered, The equation for maximum climb and take-off thrust as follows:

$$(Thr_{\text{maxclimb}})\text{ISA}=C_{T_{c,1}} \times (1 - \frac{H_p}{C_{T_{c,2}}} + C_{T_{c,3}} \times H_p{}^2) \qquad (3.23)$$

Where, $C_{T_{c,1}}$, $C_{T_{c,2}}$, and $C_{T_{c,3}}$ are climb thrust coefficient specified in the BADA tables.

The maximum climb thrust is corrected for temperature deviations from standard atmosphere, ΔT, in the following manner:

$$Thr_{\text{maxclimb}} = (Thr_{\text{maxclimb}})\text{ISA} \times (1 - C_{T_{c,5}} \times \Delta T_{eff}) \qquad (3.24)$$

Where:

$$\Delta T_{eff} = \Delta T - C_{T_{c,4}} \quad (3.25)$$

With the limits:

$$0.0 \le C_{T_{c,5}} \times \Delta T_{eff} \le 0.4 \quad (3.26)$$

And:

$$C_{T_{c,5}} \ge 0.0 \quad (3.27)$$

Where, $C_{T_{c,4}}$, and $C_{T_{c,5}}$ are thrust temperature coefficient specified in the BADA tables. This maximum climb thrust is used for both take-off and climb phases.

3.4.2 Maximum Cruise Thrust

The normal cruise thrust is by definition set equal to drag ($Thr = D$). However, the maximum amount of thrust available in cruise situation is limited. The maximum cruise thrust is calculated as a ratio of the maximum climb thrust as follows:

$$(Thr_{\text{cruise}})\text{MAX} = C_{T_{cr}} \times Thr_{\text{maxclimb}} \quad (3.28)$$

The Maximum cruise thrust coefficient $C_{T_{cr}}$ is currently uniformly set for all aircraft of value 0.95.

3.4.3 Descent Thrust

Descent thrust is calculated as a ratio of the maximum climb thrust, with different correction factors used for high and low altitudes, and approach and landing configurations, that is:

If $H_p > H_{p,des}$

$$Thr_{\text{des,high}} = C_{T_{\text{des,high}}} \times Thr_{\text{maxclimb}} \quad (3.29)$$

Where, $H_{p,des}$ is the transition altitude, $C_{T_{\text{des,high}}}$ is high altitude descent thrust coefficient specified in BADA tables.

If $H_p \leq H_{p,des}$

Cruise configuration:

$$Thr_{\text{des,low}} = C_{T_{\text{des,low}}} \times Thr_{\text{maxclimb}} \tag{3.30}$$

Where, $C_{T_{\text{des,low}}}$ is the low altitude descent thrust coefficient specified in BADA tables.

Approach configuration:

$$Thr_{\text{des,app}} = C_{T_{\text{des,app}}} \times Thr_{\text{maxclimb}} \tag{3.31}$$

Where, $C_{T_{\text{des,app}}}$ is the approach thrust coefficient specified in BADA tables.

Landing Configuration:

$$Thr_{\text{des,ld}} = C_{T_{\text{des,ld}}} \times Thr_{\text{maxclimb}} \tag{3.32}$$

Where, $C_{T_{\text{des,ld}}}$ is the landing thrust coefficient specified in BADA tables.

3.5 Fuel Consumption Model

This Subsection develops the fuel consumption model for commercial flights. In commercial flight the rate of fuel burn depends on ambient temperature, aircraft speed, and aircraft altitude. It also depend on the aircraft weight which changes as fuel burned. The Base of Aircraft Data (BADA) model provides coefficients that allows to calculate the thrust specific fuel consumption η and different thrust level Thr, which can be used to calculate the nominal fuel flow rates f_{nom} in different phases of the flight.

3.5.1 Thrust Specific Fuel Consumption

For jet engine the thrust specific fuel consumption, η [kg/ (min.KN)], is an engineering term that is used to describe the fuel efficiency of an engine design with respect to thrust output, and is specified as a function of the true airspeed, V_{TAS} [kt]:

$$\eta = C_{f_1} \times (1 + \frac{V_{TAS}}{C_{f_2}}) \tag{3.33}$$

Where, C_{f_1} , and C_{f_2} are the thrust specific fuel consumption coefficients specified in BADA tables.

3.5.2 Nominal Fuel Flow Rate

The nominal fuel flow rate, f_{nom} [kg/min], can then be calculated using the thrust:

$$f_{nom} = \eta \times Thr \tag{3.34}$$

The thrust varies with different flight phases, thus the thrust in this equation is depend on the phase which the aircraft is flying, i.e. if the aircraft is flying in climb, cruise or descent phase the thrust of this equation will be respectively climb, cruise or descent thrust. These expressions are used in all flight phases except during idle descent and cruise, where, the following expressions are to be used.

The minimum fuel flow rate, $f_{\min}$ [kg/min], corresponding to idle thrust descent conditions, is specified as a function of the geo-potential pressure altitude, H_p [ft], that is:

$$f_{\min} = C_{f_3} \times (1 - \frac{H_p}{C_{f_4}}) \tag{3.35}$$

Where, C_{f_3} , and C_{f_4} are the descent fuel flow coefficients specified in BADA tables. The idle thrust part of the descent stops when the aircraft switches to approach and landing configuration, at which point thrust is generally increased. Hence, the calculation of the fuel flow during approach and landing phases shall be based on the nominal fuel flow rate, and limited to the minimum fuel flow:

$$f_{ap/ld} = \mathrm{MAX}(f_{nom}, f_{\min}) \tag{3.36}$$

The cruise fuel flow, f_{cr} [kg/min], is calculated using the thrust specific fuel consumption, η [kg/ (min.KN)], the thrust, Thr [N], and a cruise fuel flow correction coefficient, $C_{f_{cr}}$:

$$f_{cr} = \eta \times Thr \times C_{f_{cr}} \tag{3.37}$$

For the moment the cruise fuel flow correction factor has been established for a number of aircraft types whenever the reference data for cruise fuel consumption is available. This factor has been set to 1 (one) for all the other aircraft models

For now the nominal fuel flow rate f_{nom} [kg/min], (equation 3.34) can be used for different phase of the flight, as the cruise fuel flow correction factor $C_{f_{cr}}$ has been set to 1 for most of the aircraft models, and if the thrust is not ideal during descent the fuel flow rate is based on the nominal fuel flow rate [20].

3.6 Consumed Fuel Between Waypoints

BADA defines different flight phases for a departing trajectory, with specific performance values to each phase. Thus the thrust, Thr [N] and the engine thrust specific fuel consumption, η [kg/(min.KN)], varies according to the condition verified at each flight moment. Which result different nominal fuel flows rate, f_{nom} [kg/min] for different phase of the flight. To generate a fuel optimal trajectory from a set of waypoints in 4D waypoint network requires finding the associated fuel consumed df_k by the aircraft to go from one waypoint to the other, defined as:

$$df_k = f_{nom} \times d\tau_k \tag{3.38}$$

f_{nom} [kg/min] is the nominal fuel flow rate, (equation 3.34). df_k [kg] is the amount of fuel needed from waypoints P_{k-1} to P_k and, $d\tau_k$ [min] is the amount of time needed to go from waypoints P_{k-1} to P_k. Which can be described in the following equations:

$$df_k = f_k - f_{k-1} \tag{3.39}$$

$$d\tau_k = \tau_k - \tau_{k-1} \tag{3.40}$$

Where, f_k [kg] and τ_k [min] are respectively the fuel and time required to get to waypoint P_k from initial waypoint , f_{k-1} [kg] and τ_{k-1} [min] are respectively the fuel and time required to get to waypoint P_{k-1} from initial waypoint.

Chapter 4

4 Optimal Trajectory Generation

To generate the fuel and time optimal trajectory, it is necessary to calculate the amount of consumed fuel df_k and travel time $d\tau_k$ needed between two waypoints, which was discussed In the previous chapter. Then the Dijkstra's algorithm was used to generate the fuel and time optimal trajectory by inputting these data. To generate the fuel optimal trajectory the CI assumed to be zero and the time cost was ignored and only amount of consumed fuel df_k to go from one waypoint to other was considered. In the other case, to generate the time optimal trajectory, it was assumed that the CI is maximum thus the fuel cost was ignored and only travel time $d\tau_k$ between waypoints was considered. The trajectories were generated in zero wind condition.

4.1 Selection of Flights for Analysis

For the analysis of this work short, medium and long haul 3 different flight lengths has been chosen. They are:

- Lisbon — Geneva
- Lisbon — Stockholm
- Lisbon – Montreal

Lisbon to Geneva is the short, Lisbon to Stockholm is the medium and Lisbon to Montreal is the long haul flight. Three length of flights has been chosen to compare the result of fuel consumption. The waypoints for each of the flight trajectories were chosen by the sky vector website [21]. The initial and final waypoints for the each flight were chosen at altitude 3000 feet outside of the airport, where the climb phase and landing approach begins. Firstly the waypoints were chosen by two parameters (longitude λ and latitude φ), then the altitude h of these waypoints were defined. After having the tri dimensional waypoints the arrival time τ of each waypoint calculated as described in the previous chapter. Different cruise altitude were chosen for different lengths of flight, for short, medium and long haul flight the cruise altitudes are respectively 39000 feet, 41000 feet and 43000 feet.

In each flights the 4D waypoint network consists of two different trajectories, in each trajectory, in short haul flight 10 waypoints, in medium haul flight 11 waypoints and in long haul flight 12 waypoints were chosen between the initial and final waypoints. Then the possible connection between waypoints were established in these two trajectories for each flights.

4.2 Selection of Aircraft for Analysis

The selection of aircraft types is closely linked with the flight selection. The selection of cruise altitude was also determined by the characteristics of the aircraft and the types of flight. In this work we deal with two commercial aircraft A1 and A2. For the short haul flight Lisbon to Geneva, the airplane A1 (which is a short to medium range twinjet narrow body airliner) was chosen, which has 41,000 feet of maximum altitude and nominal weight of 60,000 kg. For the medium and long haul flight Lisbon to Stockholm and Lisbon to Montreal, the airplane A2 (which is long range wide body twinjet airliner), was chosen, which has 43,100 feet of maximum altitude and nominal weight of 211,000 kg. The characteristics of airplane A1 and airplane A2 are shown in table below.

Table 4-1: Characteristics of airplane A1 and airplane A2

	Airplane A1	Airplane A2
Wing Area [m^2]	124.58	427.8
Maximum takeoff weight [kg]	70,800	287,000
Nominal weight [kg]	60,000	211,000
Cruise speed [Mach]	0.78	0.84
Maximum speed [Mach]	0.82	0.87
Maximum fuel capacity [L]	26,020	171,177
Maximum range [nm]	3,050	7,065
Engine x2	CFM 56-7 series	GE 90-94B
Thrust x2 [KN]	121	417
Maximum altitude [ft]	41,000	43,100

For the estimation of fuel consumption in each flight the nominal weight of the aircraft was considered.

4.3 Fuel Optimal Trajectory Generation

The CI (cost index) is zero in maximum range airspeed and minimum trip fuel. This speed schedule ignores the cost of time. To generate the fuel optimal trajectory, the consumed fuel df_k between waypoints were used in Dijkstra's algorithm. When trying to find a shortest (lowest cost) path for an aircraft by using Dijkstra's algorithm between two given points in space, the first step is to build a graph.

Graphs are often used to model network in which one travel from one point to another. A graph G(V, E) contains all vertices V and edges E that connect pairs of vertices. In this case of fuel optimal trajectory the waypoints are the vertices V and the consumed fuel df_k between the waypoints are the edges E.

As two different trajectories were chosen in each flight it is possible to establish connection between waypoints in these two trajectories. Once the connection has been established it is possible to calculate the consumed fuel df_k between the vertices (waypoints), which is edges between them. Then the edge (df_k) between all the vertices (waypoints) are used to build up the graph, by using this graph to Dijkstra's shortest path algorithm, the fuel optimal trajectory was generated.

4.4 Time Optimal Trajectory Generation

The maximum value for CI (cost index) uses a minimum time speed schedule. This speed schedule calls for maximum flight envelope speeds, and ignore the cost of fuel. To generate the time optimal trajectory it is needed to build a graph same as to generate the fuel optimal trajectory, but in the case of time optimal trajectory the edge of the graphs are the associated travel time $d\tau_k$ between the waypoints instead of consumed fuel df_k .

First the associated travel time $d\tau_k$ between the waypoints were calculated in each of these two trajectories, then the possible connection of waypoints between these two trajectories were established and associated travel time $d\tau_k$ between them was calculated. After that the graph was built by these vertices (waypoints) and edges ($d\tau_k$). The Dijkstra's algorithm use this graph to find the time optimal trajectory from initial waypoint to its final waypoint.

4.5 Minimization of Delay of each Waypoint in Fuel and Time Optimal Trajectories.

Once the fuel or time optimal trajectory is generated, it is possible to minimize the delay of each waypoint in the whole trajectory. Considering the trajectory have n sequence of waypoints in 4D, $P_1 = (X_1, Y_1, Z_1, \tau_1)^T$, $P_2 = (X_2, Y_2, Z_2, \tau_2)^T$,............. , $P_n = (X_n, Y_n, Z_n, \tau_n)^T$ where, X , Y , Z are the geocentric coordinates of the waypoints, and τ is the arrival time of that waypoints.

To minimize the delay at each waypoints, the trajectory is divided into segments, each segments consist of 3 waypoints, assuming the number of segment is k [k = 1,------- , (n − 2)], the segment k consist of these waypoints, P_k , P_{k+1} and P_{k+2} for time $\tau \in [\tau_k , \tau_{k+1}$ and $\tau_{k+2}]$. The geocentric coordinates X , Y , Z for different waypoints can be expressed by the following way for k segment:

$$X^k(\tau) = a_0^{\,k} + a_1^{\,k}(\tau - \tau_k) + a_2^{\,k}(\tau - \tau_k)^2 + a_3^{\,k}(\tau - \tau_k)^3 \tag{4.1}$$

$$Y^k(\tau) = b_0^{\,k} + b_1^{\,k}(\tau - \tau_k) + b_2^{\,k}(\tau - \tau_k)^2 + b_3^{\,k}(\tau - \tau_k)^3 \tag{4.2}$$

$$Z^k(\tau) = c_0^{\,k} + c_1^{\,k}(\tau - \tau_k) + c_2^{\,k}(\tau - \tau_k)^2 + c_3^{\,k}(\tau - \tau_k)^3 \tag{4.3}$$

Where, $\tau \in [\tau_k , \tau_{k+1}$ and $\tau_{k+2}]$.

Using the above equations for (n − 2) segments, it is possible to minimize the delay of each waypoints for the whole trajectory. In equations (4.1), (4.2) and (4.3) the unknowns are respectively a_0, a_1, a_2, a_3 for X coordinate, b_0, b_1, b_2, b_3 for Y coordinate and c_0, c_1, c_2, c_3 for Z coordinate. Once all the unknowns are calculated, by using these unknown coefficient it is possible to simulate the trajectory by minimizing delay in each waypoints.

4.5.1 Determination of coefficients

The unknown coefficients can be determined by the following way: For segment k=1, and $\tau = \tau_1$, from equation (4.1):

$$X^1(\tau_1) = a_0^{\,1} + a_1^{1}(\tau_1 - \tau_1) + a_2^{\,1}(\tau_1 - \tau_1)^2 + a_3^{1}(\tau_1 - \tau_1)^3 \tag{4.4}$$

So,

$$X_1 = a_0 \tag{4.5}$$

Now, the first derivatives of equation (4.4) is

$$\dot{X}^1(\tau_1) = a_1^{\,1} + 2a_2^{\,1}(\tau_1 - \tau_1) + 3a_3^{\,1}(\tau_1 - \tau_1)^2 \tag{4.6}$$

$$dX_1 = a_1 \tag{4.7}$$

Where, the initial slope of X_1 to X_2 is the following equation:

$$dX_1 = \frac{X_2 - X_1}{\tau_2 - \tau_1} \tag{4.8}$$

The value of coefficients a_0 and a_1 is found From equation (4.5) and (4.7). Now for the segment k=1 of X coordinates the unknowns are a_2 and a_3, for segment k=1 and for τ = [τ_2 , τ_3], equation (4.1) can be written as:

$$X^1(\tau_2) = a_0^{\,1} + a_1^{\,1}(\tau_2 - \tau_1) + a_2^{\,1}(\tau_2 - \tau_1)^2 + a_3^{\,1}(\tau_2 - \tau_1)^3 = X_2 \tag{4.9}$$

and,

$$X^1(\tau_3) = a_0^{\,1} + a_1^{\,1}(\tau_3 - \tau_1) + a_2^{\,1}(\tau_3 - \tau_1)^2 + a_3^{\,1}(\tau_3 - \tau_1)^3 = X_3 \tag{4.10}$$

Now by solving the equation (4.9) and (4.10), it is possible get the value of coefficient a_2 and a_3. After having all the coefficient for X coordinate for segment k=1 it is possible to simulate the trajectory of X coordinate of this segment.

To get the unknown coefficients of Y and Z coordinates in segment k=1, the same approach can be used like the X coordinates. Now calculating the unknown coefficients of X , Y , Z for all the segments k = [1,--------, (n − 2)], it is possible to simulate the whole trajectory by minimizing the delays in each waypoint.

Chapter 5

5 Simulation and Result

In this chapter the simulation and result of the fuel and time optimal trajectories are shown for three different length (short, medium and long haul) trajectories considering no wind. All the analysis of the simulation has been done using Matlab 2013[a]. The coordinates of the trajectory were chosen using skyvector website [21].

5.1 Short Haul Flight

To analyze the short haul flight, the flight from Lisbon to Geneva was considered. The initial waypoint is in 3000 feet and 14 nm away from Lisbon airport, where climb phase begins. The final waypoint also is in 3000 feet and 26 nm away from Geneva airport, where the landing approach begins.

The 4D waypoints network of this short haul flight consists of two trajectories, which has total 22 waypoints including the initial and final waypoints, and each trajectory has 12 waypoints including the initial and final waypoints. Airplane A1 was used to analyze the flight trajectories. The cruise altitude of the both trajectories is at 39000 feet. (table 5-1 and 5-2) Show the waypoints lists for both of the trajectories. Each waypoint is defined in geodetic coordinates (λ, φ, h) and their associated distance Δd_k, travel time $d\tau_k$ and consumed fuel df_k between the waypoints are also shown.

The trajectories were chosen such a way that the climb and descent phases of the first trajectory are smaller than the second trajectory but the cruise phase of the first trajectory is bigger than the second trajectory, therefore the total distance from the initial waypoint to final waypoint for both of the trajectories are more or less same.

In order to find the fuel and time optimal trajectory from the 4D waypoint network possible connection between waypoints in both trajectories were established, and their associated distance Δd_k, travel time $d\tau_k$ and consumed fuel df_k between these possible waypoints connections were calculated.

Table 5-1: List of waypoints in 1st trajectory of short haul flight

waypoint	λ [deg]	φ [deg]	h [feet]	Δd_k [nm]	$d\tau_k$ [min]	df_k [kg]
Initial (P_1)	-9.0405	38.9955	3000	0	0	0
P_2	-8.9083	39.1087	10000	9.249827	2.371751	291.0612
P_3	-8.624	39.33417	20000	19.01912	3.437191	348.0156
P_4	-7.7987	39.8783	33000	50.39803	7.295251	535.3803
P_5	-6.9993	40.2513	39000	43.16538	5.748997	294.6361
P_6	-3.3707	43.227	39000	242.0397	32.48854	1176.085
P_7	0.1303	44.729	39000	176.7117	23.71969	858.6528
P_8	3.5963	44.9543	39000	148.8367	19.97808	723.2065
P_9	3.87217	45.1205	33000	15.45767	2.058735	7.823191
P_{10}	4.6985	45.41983	20000	39.46054	5.71202	32.05871
P_{11}	5.336	45.606	10000	29.19265	5.275779	42.20624
Final (P_{22})	5.7553	45.884	3000	24.30017	5.618537	54.83692
Total				797.8314	113.7046	4363.963

Table 5-2: List of waypoints in 2nd trajectory of short haul flight

waypoint	λ [deg]	φ [deg]	h [feet]	Δd_k [nm]	$d\tau_k$ [min]	df_k [kg]
Initial (P_1)	-9.0405	38.9955	3000	0	0	0
P_{12}	-8.835	39.0883	10000	11.16491	2.862798	351.3225
P_{13}	-8.49983	39.30183	20000	20.28586	3.66612	371.1947
P_{14}	-7.59217	39.7763	33000	50.94383	7.374258	541.1783
P_{15}	-6.715	40.11317	39000	45.32355	6.036433	309.3672
P_{16}	-1.765	41.631	39000	243.352	32.6647	1182.462
P_{17}	0.5565	43.9993	39000	175.4797	23.55432	852.6664
P_{18}	3.6277	44.85317	39000	141.8812	19.04446	689.4095
P_{19}	3.9993	44.9983	33000	18.13834	2.415762	9.179894
P_{20}	4.8617	45.261	20000	39.98448	5.787862	32.48437
P_{21}	5.4975	45.5203	10000	31.13026	5.625951	45.00761
Final (P_{22})	5.7553	45.884	3000	24.40439	5.642634	55.0721
Total				802.0885	114.6753	4439.345

5.1.1 Fuel Optimal Trajectory

The fuel optimal trajectory was generated from the 4D waypoints network using the Dijkstra's shortest path algorithm, the associated consumed fuel df_k between waypoints were used as edges to find the fuel optimal trajectory.

The fuel optimal trajectory contains 9 waypoints [initial waypoint (P_1)→ P_2→ P_3→ P_4→ P_5→ P_{18}→ P_{19}→ P_{11}→ final waypoint (P_{22})], the distance between the initial and final waypoints in fuel optimal trajectory is 777.7 nm. The comparison of consumed fuel in different phases of flight for these two trajectories and fuel optimal trajectory are shown in (table 5-3).

Table 5-3: Total fuel consumed in different trajectories for short haul flight.

Trajectory	Fuel consumed [kg]			Total [kg]
	Climb	Cruise	Descent	
1	1469.1	2757.9	136.9	4363.9
2	1573.1	2724.5	141.7	4439.3
Fuel optimal	1469.1	2652.8	136.1	4258

As seen in the (table 5-3), by using the fuel optimal trajectory for the short haul flight (Lisbon – Geneva) the aircraft consumes 105.9 kg of less fuel than the first trajectory, which is equivalent to 2.4% less fuel than the first trajectory and consumes 181.3 kg of less fuel than the second trajectory, which is equivalent to 4.1% less fuel than the second trajectory. The fuel optimal trajectory in 3D is shown in (figure 5-2).

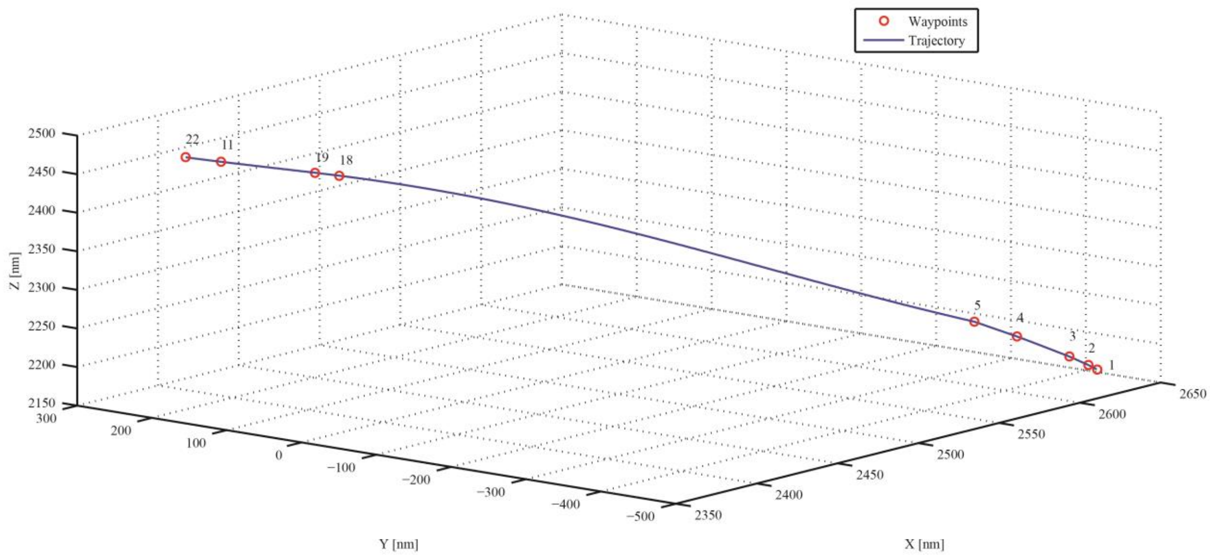

Figure 5-1: 3D fuel optimal trajectory in geocentric coordinates for short haul flight.

In figure (5-1) the curve blue line represents the real trajectory path through the different waypoints, starting on the right. The red circle around the blue line denote the position of the original waypoints.

5.1.2 Time Optimal Trajectory

The time optimal trajectory was also generated from the 4D waypoints network by using the Dijkstra's shortest path algorithm. Possible connections of waypoints between these trajectories in the waypoint network were established, then the associated time between these waypoints were used to find the time optimal trajectory.

The time optimal trajectory contains 10 waypoints [initial waypoint (P_1)→ P_2→ P_3→ P_4→ P_5→ P_8→ P_9→ P_{10}→ P_{11}→ final waypoint (P_{22})], the distance between the initial and final waypoints in the time optimal trajectory is 777.8 nm. The comparison of travel time in different phases of flight for those two trajectories and time optimal trajectory are shown in (table 5-4).

Table 5-4: Total time needed in different trajectories for short haul flight.

Trajectory	Time [min]			Total [min]
	Climb	Cruise	Descent	
1	18.9	76.2	18.7	113.7
2	19.9	75.3	19.5	114.7
Time optimal	18.9	73.49	18.7	111.01

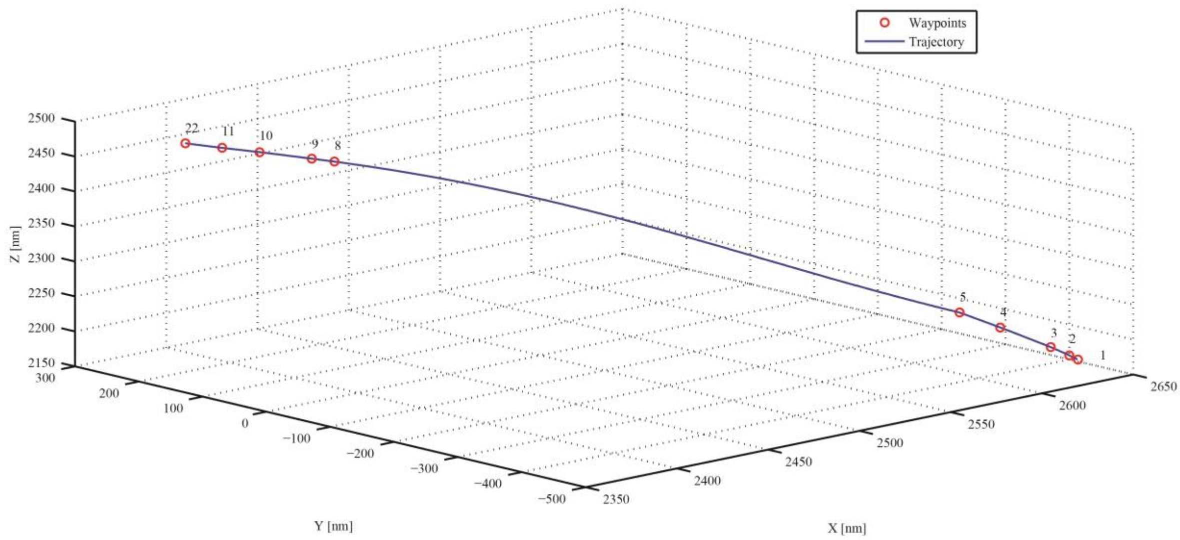

Figure 5-2: 3D time optimal trajectory in geocentric coordinates for short haul flight.

As it is seen from (table 5-4) by using the time optimal trajectory in short haul flight (Lisbon – Geneva), the aircraft reaches the final waypoint 2.7 minutes faster than the first trajectory, which is equivalent to 2.4% of total travel time of the first trajectory and 3.7 minutes faster than the second trajectory equivalent to 3.2% of total travel time of the second trajectory. The time optimal trajectory is shown in (figure 5-2), the time optimal trajectory is represented by the blue line and the red circles around the trajectories are the waypoints.

5.2 Medium Haul Flight

The flight from Lisbon to Stockholm was considered to analyze the medium haul flight. The initial waypoint is in 3000 feet and 14 nm away from Lisbon airport, where climb phase begins. The final waypoint is also in 3000 feet and 19 nm away from Stockholm Arlanda airport, where the landing approach begins.

There are two trajectories between the initial and final waypoints in the 4D waypoints network, each trajectories has 13 waypoints including the initial and final waypoints, and total 24 waypoints are there in the waypoint network including the initial and final waypoint. Airplane A2 was used to analyze the flight trajectories. The cruise altitude of the both trajectories is at 41000 feet. (table 5-5 and 5-6) Show the waypoints lists for both of the trajectories.

Table 5-5: List of waypoints in 1st trajectory of medium haul flight

waypoint	λ [deg]	φ [deg]	h [feet]	Δd_k [nm]	$d\tau_k$ [min]	df_k [kg]
Initial (P_1)	-9.0405	38.9955	3000	0	0	0
P_2	-8.9373	39.1525	10000	10.63985	2.665515	1070.631
P_3	-8.643	39.6385	24000	32.29915	5.529098	1724.94
P_4	-8.0007	40.5407	37000	61.77433	8.291856	1859.863
P_5	-7.7847	40.942	41000	26.05963	3.243938	589.0991
P_6	-4.752	46.1707	41000	340.8976	42.43539	5385.051
P_7	1.07817	49.6497	41000	314.9914	39.21055	4975.819
P_8	9.07617	53.515	41000	379.0242	47.18143	5987.324
P_9	14.4575	57.839	41000	318.0823	39.59531	5024.645
P_{10}	14.75417	58.0005	37000	13.62262	1.695762	31.54117
P_{11}	15.78983	58.624	24000	49.92285	6.807662	161.8522
P_{12}	17.0113	59.2063	10000	51.77227	9.043191	287.5735
Final (P_{24})	17.73983	59.3445	3000	23.95284	5.538229	212.0034
Total				1623.039	211.2379	27310.34

Table 5-6:List of waypoints in 2nd trajectory of medium haul flight

waypoint	λ [deg]	φ [deg]	h [feet]	Δd_k [nm]	$d\tau_k$ [min]	df_k [kg]
Initial (P_1)	-9.0405	38.9955	3000	0	0	0
P_{13}	-8.8405	39.1047	10000	11.47263	2.874146	1154.43
P_{14}	-8.455	39.576	24000	33.57806	5.748028	1793.241
P_{15}	-7.808	40.4545	37000	60.65319	8.141368	1826.109
P_{16}	-7.413	40.8377	41000	29.26358	3.642769	661.5269
P_{17}	-0.2773	44.76	41000	393.6387	49.00066	6218.184
P_{18}	4.6187	50.023	41000	374.0856	46.56667	5909.311
P_{19}	10.92483	54.85883	41000	371.7582	46.27695	5872.545
P_{20}	15.0405	57.2845	41000	201.3458	25.06379	3180.595
P_{21}	15.39	57.4757	37000	16.19891	2.016462	37.50619
P_{22}	16.496	58.17	24000	54.91818	7.488843	178.0473
P_{23}	17.504	58.94117	10000	56.26139	9.827318	312.5087
Final (P_{24})	17.73983	59.3445	3000	25.36559	5.864875	224.5074
Total				1628.54	212.5119	27368.51

5.2.1 Fuel Optimal Trajectory

The fuel optimal trajectory contains 9 waypoints [initial waypoint (P_1)→ P_2→ P_3→ P_4→ P_5→ P_{20}→ P_{21}→ P_{23}→ final waypoint (P_{24})], the distance between the initial and final waypoints in fuel optimal trajectory for this flight is 1596.5 nm. The comparison of consumed fuel in different phases of flight for different trajectories including the fuel optimal trajectory are shown in (table 5-7).

Table 5-7: Total Fuel consumed in different trajectories for medium haul flight.

Trajectory	Fuel consumed [kg]			Total [kg]
	Climb	Cruise	Descent	
1	5244.5	21372.8	692.97	27310.3
2	5435.3	21180.6	752.6	27368.5
Fuel optimal	5244.5	20744.4	742.2	26731.1

From the initial waypoint to reach the final waypoint using the fuel optimal trajectory the aircraft consumes 579.2 kg of less fuel than the first trajectory and consumes 637.4 kg of less fuel than the second trajectory. In other word by using the fuel optimal trajectory for the medium haul flight (Lisbon – Stockholm) the aircraft consumes 2.1% less fuel than the first trajectory, and 2.3% less fuel than the second trajectory. The fuel optimal trajectory is shown in (figure 5-4).

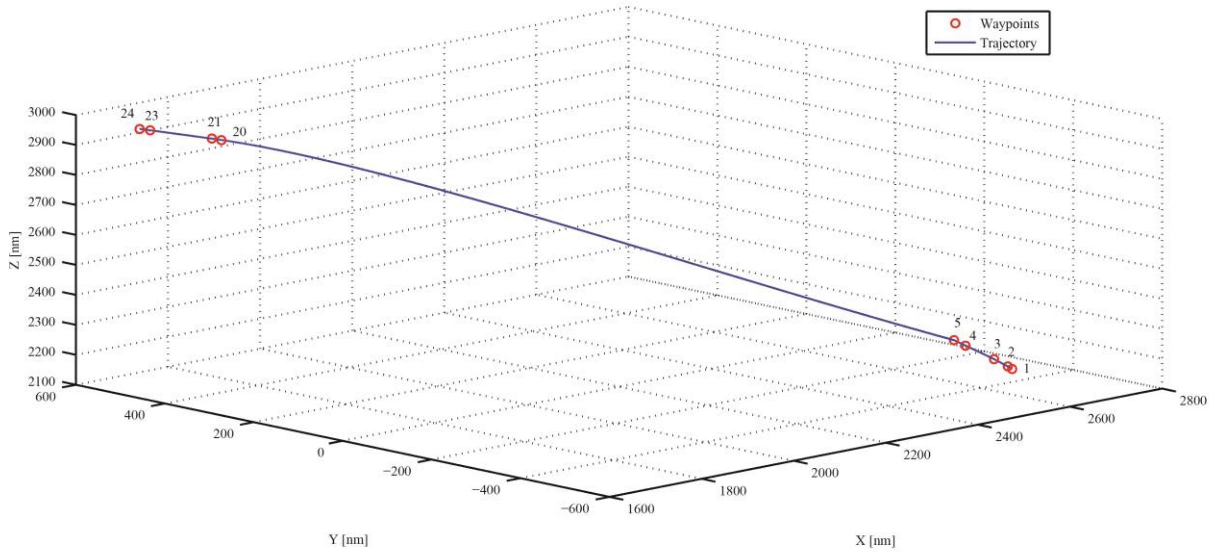

Figure 5-3: 3D fuel optimal trajectory in geocentric coordinates for medium haul flight.

The blue curve in (figure 5-3) corresponds to the fuel optimal trajectory for the medium haul flight (Lisbon – Stockholm) and the red circles around the curve are the waypoints of the fuel optimal trajectory.

5.2.2 Time Optimal Trajectory

The time optimal trajectory for the flight between Lisbon and Stockholm contains 9 waypoints [initial waypoint (P_1)→ P_2→ P_3→ P_4→ P_5→ P_9→ P_{10}→ P_{12}→ final waypoint (P_{24})], the distance between the initial and final waypoints in time optimal trajectory is 1589.6 nm. The comparison of travel time in different phases of the flight for those two trajectories and the time optimal trajectory are shown in (table 5-8).

Table 5-8: Total time needed in different trajectories for medium haul flight.

Trajectory	Time [min]			Total [min]
	Climb	Cruise	Descent	
1	19.7	168.4	23.1	211.2
2	20.4	166.9	25.2	212.5
Time optimal	19.7	164.3	23.04	207.04

By flying the time optimal trajectory in medium haul flight (Lisbon – Stockholm) 4.2 minutes or 1.9% of total travel time can be saved than the first trajectory and 5.5 minutes or 2.6% of total travel time can be saved than the second trajectory. The time optimal trajectory in 3D is shown in (figure 5-4).

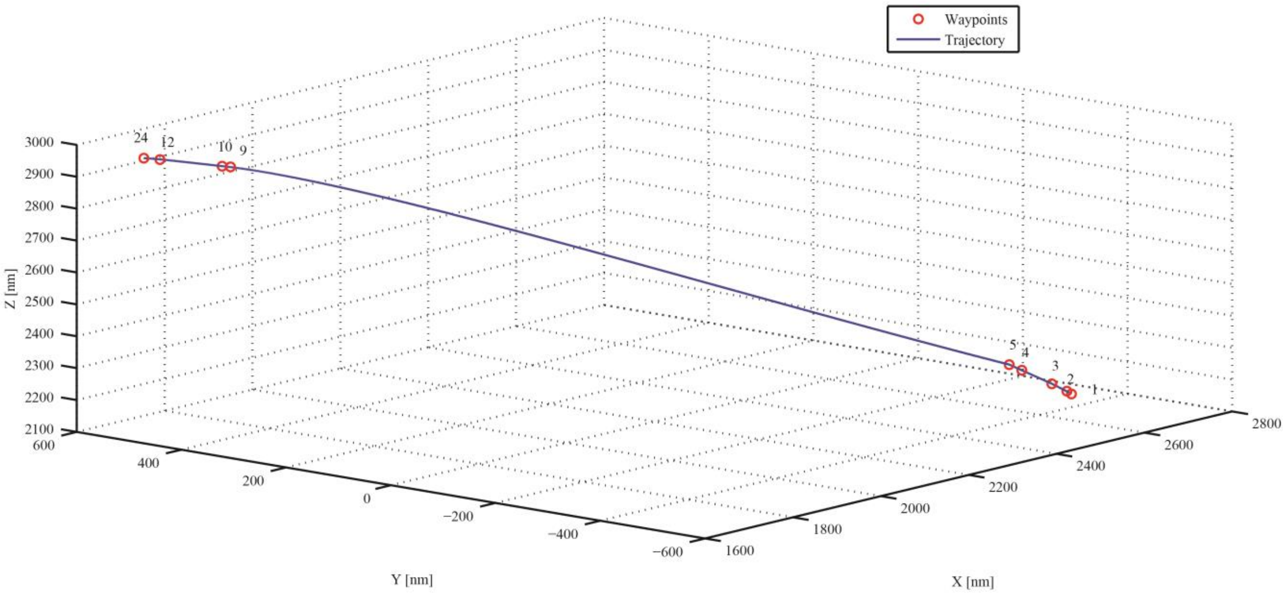

Figure 5-4: 3D time optimal trajectory in geocentric coordinates for medium haul flight.

The blue curved line is the time optimal trajectory path and the red circles around it are the associated waypoints of the time optimal trajectory.

5.3 Long Haul Flight

The flight from Lisbon to Montreal was considered to analyze the long haul flight. The initial waypoint is in 3000 feet and 14 nm away from Lisbon airport, where climb phase begins. The final waypoint is also in 3000 feet and 18 nm away from Montreal airport, where the landing approach begins.

The 4D waypoints network of the long haul flight consists of two trajectories between the initial and final waypoint, each trajectories has 14 waypoints including the initial and final waypoints, total 26 waypoints in the whole waypoint network including initial and final waypoints. Airplane A2 was used to analyze the flight trajectories. The cruise altitude of the both trajectories is at 43000 feet. The waypoints lists of both trajectories are shown in (table 5-9 and 5-10).

Table 5-9: List of waypoints in 1st trajectory of long haul flight

waypoint	λ [deg]	φ [deg]	h [feet]	Δd_k [nm]	$d\tau_k$ [min]	df_k [kg]
Initial (P_1)	-9.0405	38.9955	3000	0	0	0
P_2	-9.22083	39.1	10000	10.5683	2.64759	1063.431
P_3	-9.8425	39.3857	24000	33.76592	5.780186	1803.274
P_4	-10.9352	39.9543	37000	61.15747	8.209056	1841.291
P_5	-11.74	40.32817	43000	43.3812	5.40015	959.6066
P_6	-22.5022	43.5023	43000	518.4016	64.53132	8227.743
P_7	-35.132	44.73617	43000	550.8432	68.56969	8742.636
P_8	-44.9847	47.4295	43000	442.3112	55.05948	7020.084
P_9	-58.667	48.5647	43000	555.3268	69.12781	8813.796
P_{10}	-70.3565	46.4947	43000	491.3069	61.15854	7797.714
P_{11}	-70.809	46.4135	37000	19.45513	2.421801	43.59241
P_{12}	-71.9328	46.21	24000	48.42787	6.6038	157.0053
P_{13}	-73.0908	45.9335	10000	51.23244	8.948898	284.575
Final (P_{26})	-73.6412	45.7947	3000	24.56775	5.680405	217.4459
Total				2850.746	364.1387	46972.19

Table 5-10: List of waypoints in 2nd trajectory of long haul flight

waypoint	λ [deg]	φ [deg]	h [feet]	Δd_k [nm]	$d\tau_k$ [min]	df_k [kg]
Initial (P_1)	-9.0405	38.9955	3000	0	0	0
P_{14}	-9.2387	39.05683	10000	10.03791	2.514717	1010.061
P_{15}	-9.94583	39.2603	24000	35.28932	6.040968	1884.631
P_{16}	-11.2588	39.4515	37000	62.29715	8.362034	1875.604
P_{17}	-11.9673	39.9493	43000	44.44929	5.533107	983.2331
P_{18}	-24.8818	42.095	43000	600.2876	74.7246	9527.386
P_{19}	-34.374	43.996	43000	433.2285	53.92886	6875.93
P_{20}	-44.3497	46.44083	43000	448.0273	55.77103	7110.806
P_{21}	-61.77	47.44	43000	717.2308	89.28184	11383.43
P_{22}	-70.163	46.2543	43000	353.4368	43.99628	5609.525
P_{23}	-70.557	46.102	37000	18.61899	2.317716	41.71889
P_{24}	-71.739	45.9043	24000	51.21564	6.98395	166.0434
P_{25}	-72.9952	45.81	10000	53.07175	9.270174	294.7915
Final (P_{26})	-73.6412	45.7947	3000	27.16449	6.280807	240.4293
Total				2854.355	365.0061	47003.6

5.3.1 Fuel Optimal Trajectory

The fuel optimal trajectory of the flight between Lisbon and Montreal contains 9 waypoints [initial waypoint (P_1)→ P_{14}→ P_3→ P_4→ P_5→ P_{22}→ P_{11}→ P_{13}→ final waypoint (P_{26})], the distance between the initial and final waypoints in fuel optimal trajectory is 2777 nm. The comparison of consumed fuel in different phases of flight for different trajectories and the fuel optimal trajectory are shown in (table 5-11).

Table 5-11: Total Fuel consumed in different trajectories for long haul flight.

Trajectory	Fuel consumed [kg]			Total [kg]
	Climb	Cruise	Descent	
1	5667.6	40601.9	702.6	46972.2
2	5753.5	40507.1	742.98	47003.6
Fuel optimal	5652.1	39284.9	712.5	45649.5

Using the fuel optimal trajectory in long haul flight (Lisbon – Montreal) the aircraft consumed 1322.7 kg of less fuel than the first trajectory and consumed 1354.1 kg less fuel than the second trajectory. So in another word by flying the fuel optimal trajectory for the long haul flight the aircraft consumes 2.8% less fuel than the first trajectory, and 2.9% less fuel than the second trajectory. The fuel optimal trajectory in 3D is shown in (figure 5-5).

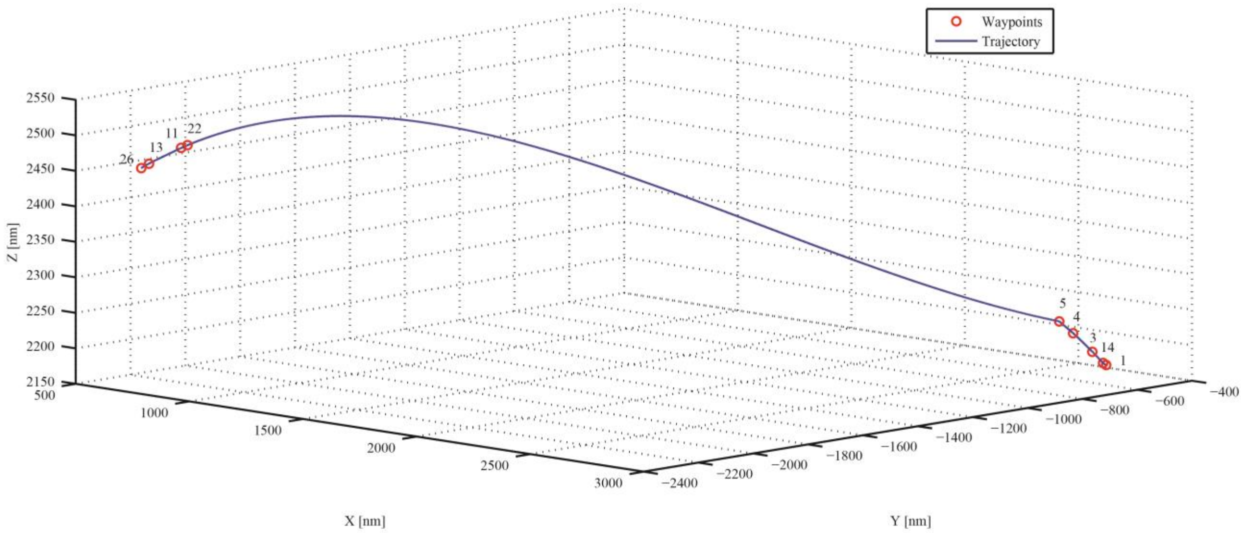

Figure 5-5: 3D fuel optimal trajectory in geocentric coordinates for long haul flight.

The blue curve in the (figure 5-5) is the fuel optimal trajectory and the red circles around it are the waypoints of that trajectory. In this long haul flight the cruise phase is really large compare to its climb and descent phases, thus in the figure the waypoints in the climb and descent phases are seems too close to each other.

5.3.2 Time Optimal Trajectory

The time optimal trajectory of flight between Lisbon to Montreal contains 9 waypoints [initial waypoint (P_1)→ P_{14}→ P_3→ P_4→ P_5→ P_{10}→ P_{11}→ P_{13}→ final waypoint (P_{26})], the distance between the initial and final waypoints in time optimal trajectory of this flight is 2772 nm. The comparison of travel time in different phases of flight for different trajectories and time optimal trajectory are shown in (table 5-12).

Table 5-12: Total time needed in different trajectories for long haul flight.

Trajectory	Time [min]			Total [min]
	Climb	Cruise	Descent	
1	22.04	318.5	23.7	364.2
2	22.5	317.7	24.9	365.1
Time optimal	22.03	308.6	23.6	354.3

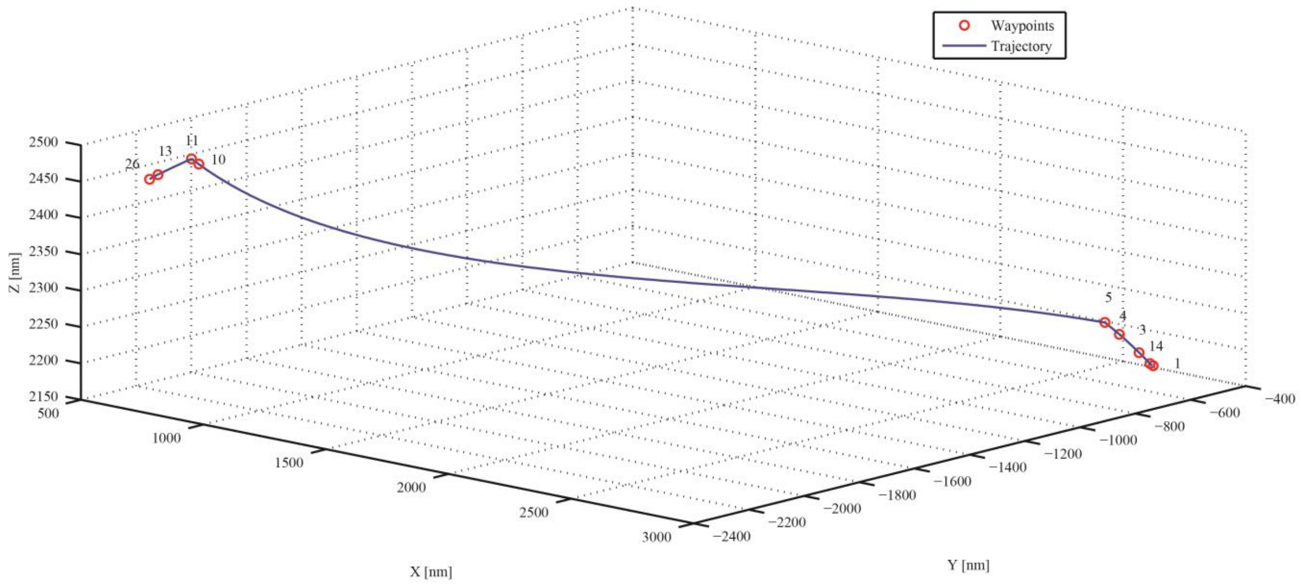

Figure 5-6: 3D fuel optimal trajectory in geocentric coordinates for long haul flight.

By using the time optimal trajectory in long haul flight (Lisbon – Montreal) the aircraft reaches to the final waypoint from the initial waypoint 9.9 minutes faster than the first trajectory which saves 2.7% of the total travel time and 10.8 minutes faster than the second trajectory which save 2.9% of total travel time. The time optimal trajectory in 3D is shown in (figure 5-6).

In the (figure 5-6) the blue curve is the time optimal trajectory and the red circles around it are the waypoints of the trajectory. In the time optimal trajectory the cruise phase of the flight is really large compare to its climb and descent phases, thus in the figure the waypoints in the climb and descent phases are seems too close to each other.

Chapter 6

6 Conclusion and Discussions

This study is based on finding the fuel and time optimal trajectories of climb, cruise and descent phases of the flight, without the takeoff and landing phases of the flight. In this work several steps were made in order to achieve a complete trajectory from 4D waypoint networks that minimizes the fuel consumption and travel time. This study uses Dijkstra’s shortest path algorithm that finds the shortest path in a graph, which is refers to a collection of vertices (waypoints) and a collection of edges (associated consumed fuel or travel time) that connect the pairs of vertices. This technique was used to compare different length (short, medium and long haul) flights.

The analysis results show promising potential for reduction of consumed fuel and travel time in different flights via using the Dijkstra’s shortest path algorithm, across a range of common aircraft and routes. The results suggest that by flying fuel and time optimal trajectory for short haul flight, it is possible to save 2.4—4.1% on fuel burn, which is equivalent to 105.9 – 181.3 kilograms of fuel and 2.7—3.7 minutes or 2.4 - 3.2 % of total travel time. In medium haul flight by flying the fuel optimal trajectory can potentially save 2.1—2.3% fuel, reducing fuel burn by 579.2 – 637.4 kilograms and by flying the time optimal trajectory the travel time was reduced by 4.2—5.5 minutes or 1.9 – 2.6% of total travel time. For long haul flight it is possible to save 2.8—2.9% on fuel burn, which is equivalent to 1322.7 – 1354.1 kilogram of fuel by flying the fuel optimal trajectory, and 9.9—10.8 minutes or 2.7 -2.9% of total travel time was saved by flying the time optimal trajectory. In general the savings of the fuel and time are proportional to the trip lengths, and depends on the aircraft types.

The results show that during the cruise phase, the aircraft consumes the majority of fuel but fuel consumption per unit time is higher during the climb phase and in descent phase the fuel consumption per unit time is smaller than the other two phases. So for the fuel optimal trajectory the algorithm tries to obtain the trajectory by choosing short climb and cruise phases and long descent phase.

6.1 Future work

Although the algorithm has proven reliable to find the fuel and time optimal trajectory from 4D waypoint networks, there is still room for improvement. By using more trajectories and networks with different cruise altitude more fuel and time can be saved, as there will be more waypoints to choose from.

In addition, a realistic wind model and Air traffic control (ATC) restrictions can be imposed on the 4D waypoints network to find the fuel and time optimal trajectory in presence of wind and other source of disturbances to model more realistic flight.

7 References

[1] ICAO, "ICAO Environmental Report: Aviation and Climate change," *ICAO*, 2013.

[2] Penner J. E, Lister D. H, Griggs D. J, Dokken D. J and McFarland M, "Aviation and the Global Atmosphere," *Intergovernmental Panel on Climate Change*, 1999.

[3] S. W. airlines, "Fuel Savings: Reducing Our Environmental Impact," [Online]. Available: https://www.southwest.com/html/southwest-difference/southwest-citizenship/environmental-initiatives/. [Accessed June 2015].

[4] C. P. airlines, "Cathay Pacific “silver bullet” freighter takes to the skies," [Online]. Available: http://centreforaviation.com/analysis/cathay-pacific-silver-bullet-freighter-takes-to-the-skies-4553. [Accessed June 2015].

[5] Roberson B, "Fuel Conservation Strategies: Cost Index Explained," *Boeing*, 2007, pp 26-28.

[6] Airbus, "Getting to grips with fuel economy," *Airbus*, October 2004.

[7] Roberson W, Root R and Adams D, "Fuel Conservation strategies : Cruise Flight," *Boeing*, 2007, pp 23-27.

[8] Roberson W and Johns J. A, "Fuel Conservation Strategies: Takeoff and Climb," *Boeing*, 2008, pp 25-28.

[9] Allison R. L, "Application of NASA-ARC delayed flap approach procedure to Boeing 727 Airplane," *NASA*, February 1977.

[10] Roberson W and Johns j. A, "Fuel Conservation Stategies: Descent and Approach," *Boeing*, 2008, pp 25-28.

[11] Bryson A. E and Ho Y. C, "*Applied Optimal Control: Optimization, Estimation and, Control*", Taylor & Francis, New York, 1975, pp. 42-89.

[12] Calise A," Extended Energy Management for Flight Performance Optimization", *AIAA Journal*, VOl. 15, No. 3, March 1977, pp. 314-321.

[13] Calise A and Moerder D, "Singular Perturbation Techniques for Real Time Aircraft Trajectory Optimization and Control", *NASA CR-3597*, 1982.

[14] Cormen T. H, Leiserson C. E, Rivest R. L and Stein C, "*Introduction to algorithms*", London, England: The MIT press, 2009, pp. 658-659.

[15] Hart C, "Graph Theory Topics in Computer Networking," 2013, pp 13-20.

[16] Dasgupta S, Papadimitriou C. H and Vazirani U. V, "*Algorithms*", McGraw-Hill, New York, July 18, 2006, pp. 112-118.

[17] Machado P and Bousson K, "4D Flight Trajectory Optimization Based on Pseudospectral Methods," *WSEAS transactions on system and control*, Vol 8, No 3, july 2013, pp 105-119.

[18] Seemkooei A. A, "Comparison of different algorithm to transform geocentric to geodetic coordinates," *Survey Review 36*, October 2002, pp 627-632.

[19] EUROCONTROL "Aircraft Performance Summary Tables for the Base of Aircraft Data (BADA)," *Eurocontrol Experimental Centre*, Revision 3.4, June 2002,.

[20] EUROCONTROL, "User manual for the base of aircraft data (BADA) revision 3.9," *Eurocontrol Experimental Centre*, Revision 3.4, April 2011.

[21] "SkyVector," [Online]. Available: https://skyvector.com/. [Accessed October 2015].

Annex A – Results

Short Haul Flight

Fuel Optimal Trajectory

waypoint	λ [deg]	φ [deg]	h [feet]	Δd_k [nm]	$d\tau_k$ [min]	df_k [kg]
Initial (P_1)	-9.0405	38.9955	3000	0	0	0
P_2	-8.9083	39.1087	10000	9.24982731	2.371750592	291.0612327
P_3	-8.624	39.33417	20000	19.01912267	3.437190843	348.0155729
P_4	-7.7987	39.8783	33000	50.39802743	7.295251257	535.3802516
P_5	-6.9993	40.2513	39000	43.16538208	5.748996503	294.6360708
P_{18}	3.6277	44.85317	39000	545.9488459	73.28172428	2652.798419
P_{19}	3.9993	44.9983	33000	18.13834289	2.41576154	9.179893851
P_{11}	5.336	45.606	10000	67.50872653	10.90315906	72.04807509
Final (P_{22})	5.7553	45.884	3000	24.3001715	5.618536764	54.83691882
Total				777.7284463	111.0723708	4257.956435

Time Optimal Trajectory

waypoint	λ [deg]	φ [deg]	h [feet]	Δd_k [nm]	$d\tau_k$ [min]	df_k [kg]
Initial (P_1)	-9.0405	38.9955	3000	0	0	0
P_2	-8.9083	39.1087	10000	9.24982731	2.371750592	291.0612327
P_3	-8.624	39.33417	20000	19.01912267	3.437190843	348.0155729
P_4	-7.7987	39.8783	33000	50.39802743	7.295251257	535.3802516
P_5	-6.9993	40.2513	39000	43.16538208	5.748996503	294.6360708
P_8	3.5963	44.9543	39000	547.5123329	73.49158831	2660.395497
P_9	3.87217	45.1205	33000	15.45766508	2.058734528	7.823191205
P_{10}	4.6985	45.419833	20000	39.46053795	5.712019968	32.05871207
P_{11}	5.336	45.606	10000	29.19264614	5.275779423	42.20623539
Final (P_{22})	5.7553	45.884	3000	24.3001715	5.618536764	54.83691882
Total				777.7557131	111.0098482	4266.413682

Medium Haul Flight

Fuel Optimal Trajectory

waypoint	λ [deg]	φ [deg]	h [feet]	Δd_k [nm]	$d\tau_k$ [min]	df_k [kg]
Initial (P_1)	-9.0405	38.9955	3000	0	0	0
P_2	-8.9373	39.1525	10000	10.63984735	2.665514994	1070.630752
P_3	-8.643	39.6385	24000	32.2991454	5.529097643	1724.940237
P_4	-8.0007	40.5407	37000	61.77432604	8.291855844	1859.863266
P_5	-7.7847	40.942	41000	26.05963408	3.243937852	589.099114
P_{20}	15.0405	57.2845	41000	1313.210885	163.4702346	20744.37277
P_{21}	15.39	57.4757	37000	16.19890882	2.016461679	37.50618723
P_{23}	17.504	58.94117	10000	110.97267	17.27201089	480.1619027
Final (P_{24})	17.73983	59.3445	3000	25.36558534	5.864875223	224.5074236
Total				1596.521002	208.3539887	26731.08165

Time Optimal Trajectory

waypoint	λ [deg]	φ [deg]	h [feet]	Δd_k [nm]	$d\tau_k$ [min]	df_k [kg]
Initial (P_1)	-9.0405	38.9955	3000	0	0	0
P_2	-8.9373	39.1525	10000	10.63984735	2.665514994	1070.630752
P_3	-8.643	39.6385	24000	32.2991454	5.529097643	1724.940237
P_4	-8.0007	40.5407	37000	61.77432604	8.291855844	1859.863266
P_5	-7.7847	40.942	41000	26.05963408	3.243937852	589.099114
P_9	14.4575	57.839	41000	1319.621296	164.2682112	20845.636
P_{10}	14.75417	58.0005	37000	13.62262133	1.695761991	31.54117304
P_{12}	17.0113	59.2063	10000	101.5868205	15.8111783	439.5507566
Final (P_{24})	17.73983	59.3445	3000	23.95284067	5.538229057	212.0034083
Total				1589.556532	207.0437869	26773.26471

Long Haul Flight

Fuel Optimal Trajectory

waypoint	λ [deg]	φ [deg]	h [feet]	Δd_k [nm]	$d\tau_k$ [min]	df_k [kg]
Initial (P_1)	-9.0405	38.9955	3000	0	0	0
P_{14}	-9.2387	39.05683	10000	10.0379116	2.514716893	1010.061187
P_3	-9.8425	39.3857	24000	34.47508776	5.90158421	1841.146734
P_4	-10.93517	39.9543	37000	61.15746523	8.209055735	1841.291201
P_5	-11.74	40.32817	43000	43.38120141	5.400149554	959.6065757
P_{22}	-70.163	46.2543	43000	2475.208848	308.117284	39284.95371
P_{11}	-70.809	46.4135	37000	28.56382277	3.555662585	64.00192654
P_{13}	-73.09083	45.9335	10000	99.61194468	15.50380462	431.0057684
Final (P_{26})	-73.64117	45.7947	3000	24.56775255	5.680405215	217.4459116
Total				2777.004034	354.8826628	45649.51302

Time Optimal Trajectory

waypoint	λ [deg]	φ [deg]	h [feet]	Δd_k [nm]	$d\tau_k$ [min]	df_k [kg]
Initial (P_1)	-9.0405	38.9955	3000	0	0	0
P_{14}	-9.2387	39.05683	10000	10.0379116	2.514716893	1010.061187
P_3	-9.8425	39.3857	24000	34.47508776	5.90158421	1841.146734
P_4	-10.93517	39.9543	37000	61.15746523	8.209055735	1841.291201
P_5	-11.74	40.32817	43000	43.38120141	5.400149554	959.6065757
P_{10}	-70.3565	46.4947	43000	2479.302175	308.6268268	39349.92041
P_{11}	-70.809	46.4135	37000	19.45513208	2.421800673	43.59241212
P_{13}	-73.09083	45.9335	10000	99.61194468	15.50380462	431.0057684
Final (P_{26})	-73.64117	45.7947	3000	24.56775255	5.680405215	217.4459116
Total				2771.98867	354.2583437	45694.0702

Annex B - Article "Optimal Fuel Conservation in 4D Waypoint Networks"

(Submitted to a refereed journal listed in the ISI Journal Citation Reports)

Optimal Fuel Conservation in 4D Waypoint Networks

Kawser Ahmed[1]

Department of Aerospace Science, University of Beira Interior, Covilhã, Portugal

Abstract

The purpose of this work is to develop a trajectory optimization algorithm that finds a fuel optimal trajectory from a 4D waypoint networks, where the arrival time is specified for each waypoint in the networks. A single source shortest path algorithm is presented to generate the optimal aircraft trajectory that minimizes fuel burn, generating such trajectory helps the aviation industry cope with increasing fuel costs and reduce aviation induced climate change, as CO_2 is directly related to the amount of fuel burned, reduction in fuel burn implies a reduction in carbon emissions as well. Results of this work shows that by flying a fuel optimal trajectory, which was found by implying a single source shortest path algorithm (Dijkstra's algorithm) can lead to reduction of average fuel burn of international flights by 2.8% of the total trip fuel.

Key words: Fuel Conservation; Cost Index; 4D trajectories; Dijkstra's algorithm; Waypoint navigation; Base of Aircraft Data (BADA);

1. Introduction

Improving aircraft operational efficiency has become a dominant theme in air transportation, as the airlines around the world have seen the price of fuel has risen sharply during the last decades. Currently, aviation accounts for about 2% of total global CO_2 emissions and about 12% of the CO_2 from all transportation source [1]. This increased fuel prices and environmental concerns have pushed airlines to reduce fuel consumption and to find margins for performance improvements. Efforts to modernize

1

the aircraft fleet are limited by extremely slow and expensive process of new aircraft adoption, which can take decades, therefore it is important to find different alternatives to reduce the fuel consumption in current aircrafts, which will likely to share the sky with most modern aircraft in near future. One of these alternatives is to optimize flight trajectories and traffic control procedure. The existing flight planning techniques are suboptimal. Hence, a fuel optimal flight path can significantly save fuel.

A practical solution that reduces the cost associated with time and fuel consumption during flight is the Cost Index (CI). The value of the CI reflects the relative effects of fuel cost on overall trip cost as compared to time-related direct operating cost. For all the aircraft models, the minimum value of cost index equal to zero results in maximum range airspeed and minimum trip fuel, but this configuration ignores the time cost. If the cost index is maximum, the flight time is minimum, the velocity and the Mach number are maximum, but ignores the fuel cost [2]. In this study the Cost Index assumes to be zero as only fuel cost is taken into consideration.

$$CI = \frac{TimeCost \sim (€/hr)}{FuelCost \sim (€/kg)} \tag{1}$$

Recent studies propose that, during the takeoff and climb phase of the flight, accelerating and flap retraction at a lower altitude than the typical 3000 ft decrease the fuel consumption, lower flap setting cause low drag, resulting less fuel burn during climb, it also suggest that descending at a higher slope angle than 3^0 enable the aircraft to save fuel [3], [4]. By improving the cruise speed and altitude profiles is possible to reduce fuel burn in cruise phase, Patrick Hagelauer and Felix Mora camino conducted a study based on a constant value of Cost Index for a given arrival time, in order to find the optimum cruise speed and altitude profile [5].

Classical aircraft trajectory optimizations are solved by applying calculus of variations to determine the optimality conditions, requiring the solution of non-linear Two-Point Boundary Value Problems (TPBVPs) [6]. Alternatively, a more general solution to aircraft trajectory optimization can be obtained by singular perturbation theory which approximates solutions of high order problems by the solution of a series of lower order systems with the system dynamics separated into low and fast modes [7], [8].

With the tremendous advancement in numerical computing power, TPBVPs can be converted to nonlinear programming problems that are solvable even for problems with many variables and constraints using numerical algorithms such as direct collocation methods. Neglecting aircraft dynamics and applying shortest path algorithms in graph theory, an optimal trajectory can be approximated by the path that minimizes the total link cost connecting the origin and destination in a pre-defined network. The graph methods often require large computation time and memory space but guarantee global optimal solutions. In this paper the single source shortest path algorithm was used to generate the fuel optimal trajectory.

This study is restricted to the climb, cruise and descent phases of the flight and ignores the takeoff and landing approach, and assuming the initial and final waypoints are at altitude of 3000 feet, where in the initial waypoint the aircraft begins the climb phase and in the final waypoint the aircraft begins the landing approach. This work primarily attempts to quantify benefits of fuel optimal trajectory which was found by implying the Dijkstra's shortest path algorithm, a benefit is meant to imply a reduction in fuel burn due to using the Dijkstra's shortest path algorithm to the actual unimproved flight.

2. Problem Statement

The main goal of this paper is to find a fuel optimal path from a 4D waypoint networks. Most of the approaches consider the waypoints defined by tridimensional coordinate positions $P_k = (\lambda_k, \varphi_k, h_k)^T$ $k = 1,2,\ldots,N$ and do not take into account the time. By adding the arrival time restriction to the tri-dimensional waypoint it is possible to define the 4D waypoints as $P_k = (\lambda_k, \varphi_k, h_k, \tau_k)^T$. Where: $\lambda_k, \varphi_k, h_k, \tau_k$ is respectively longitude, latitude, altitude and arrival time at waypoint P_k.

The problem to be solved is to estimate associated travel time $d\tau_k$ and consumed fuel df_k between the waypoints in the 4D waypoint networks, then to use the value of associated consumed fuel df_k between waypoints as edges and the waypoints as vertices in Dijkstra's algorithm to find the fuel optimal trajectory from initial waypoint to final waypoint from the 4D waypoint networks.

The following section propose a method that will determine the fuel optimal path along specified waypoints from a 4D waypoint networks by implying the Dijkstra's shortest path algorithm.

3. Proposed Method

To generate an fuel optimal trajectory from a set of waypoints in 4D waypoint networks requires finding the associated fuel consumed df_k by the aircraft to go from one waypoint to the other, defined as:

$$df_k = f_{nom} \times d\tau_k \tag{2}$$

Where, f_{nom} [kg/min] is the nominal fuel flow rate, df_k [kg] is the amount of fuel consumed by the aircraft to go from waypoints P_{k-1} to P_k and, $d\tau_k$ [min] is the amount of time needed to go from waypoints P_{k-1} to P_k. Which can be described in the following equations:

$$df_k = f_k - f_{k-1} \tag{3}$$

$$d\tau_k = \tau_k - \tau_{k-1} \tag{4}$$

Where, f_k [kg] and τ_k [min] are respectively the fuel and time required to get to waypoint P_k from initial waypoint, f_{k-1} [kg] and τ_{k-1} [min] are respectively the fuel and time required to get to waypoint P_{k-1} from initial waypoint.

3.1 Dijkstra's Algorithm

Dijkstra's algorithm is a simple greedy algorithm to solve single source shortest paths problem. For a given source vertex in the graph, the algorithm finds the path with lowest cost (i.e. the shortest path) between that vertex and every other vertex [9] [10] [11]. It require three inputs (G, w, s) they are the graph G, the weights w, and the source vertex s. Graphs are often used to model networks in which one travels from one point to another. A graph G (V, E) refers to a collection of vertices V and a collection of edges E that connect pairs of vertices and assuming all edges cost are non-negative, thus there are no negative cycles and shortest paths exists for all vertices reachable from source vertex s. In this work the waypoints of the 4D waypoint networks are the vertices, the initial waypoint is the source vertex, the final waypoint is the destination vertex and the consumed fuel df_k by the aircraft between the pairs of waypoints are the edges between these vertices (waypoints).

3.2 Modeling of 4D Waypoints Networks

Suppose the waypoints networks consists of N sets of waypoints, where P_1 is the initial waypoint and P_N is the final waypoint. Each waypoint P_k, (*k =1,2,…., N*) is defined by the geodetic coordinates $\lambda_k, \varphi_k, h_k$, by considering the arrival time in each waypoint τ_k, the waypoint P_k can be described as a four-dimensional state vector:

$$P_k = (\lambda_k, \varphi_k, h_k, \tau_k)^T \tag{5}$$

Where, λ_k and φ_k are the longitude and latitude of waypoint P_k, h_k is the altitude (with respect to sea level). The following subsections represent the navigation model and constraints of 4D waypoints networks.

3.2.1 Navigation Model

The following differential equations model the dynamics of the navigation process:

$$\dot{\lambda} = \frac{V \cos\gamma \sin\psi}{(R_e + h)\cos\varphi} \tag{6}$$

$$\dot{\varphi} = \frac{V \cos\gamma \cos\psi}{(R_e + h)} \tag{7}$$

$$\dot{h} = V \sin\gamma \tag{8}$$

$$\dot{V} = u_1 \tag{9}$$

$$\dot{\gamma} = u_2 \tag{10}$$

$$\dot{\psi} = u_3 \tag{11}$$

Where, V = flight velocity, γ = flight path angle, ψ =heading (with respect to the geographical north), λ = longitude, φ = latitude, h = the altitude (with respect to sea level), R_e is the Earth radius. The variables u_1, u_2, and u_3 are respectively the acceleration, the flight path angle rate and the heading rate. The state vector x and control vector u of the above model are described respectively as:

$$x = (\lambda, \varphi, h, V, \gamma, \psi)^T \tag{12}$$

$$u = (u_1, u_2, u_3)^T \tag{13}$$

3.2.2 Navigation Constraints

The real world flight operate under several constraints, due to aircraft performance, aerodynamic structural limits, safety reasons, the mission and other factor.

$$a_{\min} \le a \le a_{\max} \tag{14}$$

$$\gamma_{\min} \le \gamma \le \gamma_{\max} \tag{15}$$

$$V_{\min} \le V \le V_{\max} \tag{16}$$

3.3 Arrival Time of Each Waypoint

The 4D navigation consists of traveling through a sequence of predefined waypoints in a given time of flight, which in turn define the trajectory of the flight. Assuming that the waypoint P_k is already defined by the geodetic coordinates longitude λ_k, latitude φ_k, and altitude h_k, where the scheduled time of arrival τ_k at this waypoint is unknown. To compute this unknown arrival time of each waypoint, the distance between this waypoint and its previous waypoint from where the aircraft is arriving and the average velocity of the aircraft between this two waypoints is required.

The trajectory generation requires a geocentric coordinates system. To calculate the distance between two waypoints, the 3D waypoint need to be transformed from usual geodetic coordinates system to geocentric coordinates system. The 3D waypoint P_k is defined by the following way:

$$P_k = (\lambda_k, \varphi_k, h_k)^T \tag{17}$$

Now to transform these geodetic coordinates to geocentric coordinates, the following equations are required [12].

$$X_k = (N_k + h_k)\cos\varphi_k \cos\lambda_k \tag{18}$$

$$Y_k = (N_k + h_k)\cos\varphi_k \sin\lambda_k \tag{19}$$

$$Z_k = [N_k(1-e^2) + h_k]\sin\varphi_k \tag{20}$$

Being a is the Earth semi major axis and e its eccentricity, N_k can be calculated as follows:

$$N_k = \frac{a}{\sqrt{1-e^2\sin^2\varphi_k}} \tag{21}$$

After transforming the 3D waypoint from geodetic coordinates to geocentric coordinates system, Now it is possible to calculate Δd_k (the distance between two waypoints P_{k-1} to P_k) by using the following equation:

$$\Delta d_k = \sqrt{(X_k - X_{k-1})^2 + (Y_k - Y_{k-1})^2 + (Z_k - Z_{k-1})^2} \tag{22}$$

To estimate the appropriate velocity of the aircraft V_k at any waypoint P_k, the following equation can be used:

$$V_k = \sqrt{\frac{2W}{\rho_k C_L S}} \tag{23}$$

Where, W is the aircraft nominal weight, C_L is the lift coefficient, S is the wing area of the aircraft and ρ_k is the air density (varies with altitude) at waypoint P_k. It is possible to get the appropriate velocity at any waypoint P_k from Base of Aircraft Data (BADA), where true air speed, V_{TAS} [kt] is specified for different aircraft for different flight level and phases of the flights [13].

By using the distance between two waypoints and the velocity of the aircraft in both waypoints the arrival time of each waypoint can be computed as follow:

$$d\tau_k = \frac{\Delta d_k}{\frac{V_k + V_{k-1}}{2}} \tag{24}$$

Where, $d\tau_k$ is the time needed to go from waypoint P_{k-1} to P_k. So the arrival time of waypoint P_k from the initial waypoint can be described as follow:

$$\tau_k = \tau_{k-1} + d\tau_k \tag{25}$$

In practice, the aircraft may not pass through the waypoint P_k exactly at this specified time τ_k due to disturbances. Therefore, an appropriate way is rather imposing a time tolerance ε in (equation 25).

$$\tau_k = \tau_{k-1} + \varepsilon \times d\tau_k \tag{26}$$

Where, ε is the tolerance time interval for arrival at a determined waypoint [$1.0 \leq \epsilon \leq 1.4$], if the altitude of waypoints P_{k-1} and P_k are same, then the tolerance ϵ can be assumed 1.

3.4 Fuel Consumption Model

This Subsection develops the fuel consumption model for commercial flights. In commercial flight the rate of fuel burn depends on ambient temperature, aircraft speed, and aircraft altitude. It also depend on the aircraft weight which changes as fuel burned. The Base of Aircraft Data (BADA) model provides coefficients that allows to calculate the thrust specific fuel consumption η and different thrust level Thr, which can be used to calculate the nominal fuel flow rates f_{nom} in different phase of the flight [14].

3.4.1 Nominal Fuel Flow Rate

The nominal fuel flow rate, f_{nom} [kg/min], can be calculated using the thrust and thrust specific fuel consumption as follows:

$$f_{nom} = \eta \times Thr \qquad (27)$$

The thrust varies with different flight phases, thus the thrust in (equation 27) depends on the phase which the aircraft is flying, i.e. if the aircraft is flying in climb, cruise or descent phase the thrust of this equation will be respectively climb, cruise or descent thrust. The thrust specific fuel consumption η and different thrust level Thr are explained in the following subsections. This expression can be used in all flight phases except during idle descent and cruise, where, the following expressions are to be used.

The minimum fuel flow rate, $f_{\min}$ [kg/min], corresponding to idle thrust descent conditions, is specified as a function of the geo-potential pressure altitude, H_p [ft], that is:

$$f_{\min} = C_{f_3} \times (1 - \frac{H_p}{C_{f_4}}) \qquad (28)$$

Where, C_{f_3} and C_{f_4} are the descent fuel flow coefficients specified in BADA tables. The idle thrust part of the descent stops when the aircraft switches to approach and landing configuration, at this point thrust is generally increased. Hence, the calculation of the fuel flow during approach and landing phases shall be based on the nominal fuel flow rate, and limited to the minimum fuel flow:

$$f_{ap/ld} = \mathrm{MAX}(f_{nom}, f_{\min}) \tag{29}$$

To calculate the cruise fuel flow rate, f_{cr} [kg/min], a cruise fuel flow correction coefficient, $C_{f_{cr}}$ is needed with the thrust specific fuel consumption, η [kg/ (min.KN)] and the thrust, Thr [N],which can be expressed in the following form:

$$f_{cr} = \eta \times Thr \times C_{f_{cr}} \tag{30}$$

For the moment the cruise fuel flow correction factor has been established for a number of aircraft types whenever the reference data for cruise fuel consumption is available. This factor has been set to 1 for all the other aircraft models.

For now the nominal fuel flow rate f_{nom} [kg/min], (equation27) can be used for different phase of the flight, as the cruise fuel flow correction factor $C_{f_{cr}}$ has been set to 1 for most of the aircraft models, and if the thrust is not ideal during descent the fuel flow rate is based on the nominal fuel flow rate.

3.4.2 Thrust Specific Fuel Consumption

For jet engine the thrust specific fuel consumption, η [kg/ (min.KN)], is an engineering term that is used to describe the fuel efficiency of an engine design with respect to thrust output, and is specified as a function of the true airspeed, V_{TAS} [kt]:

$$\eta = C_{f_1} \times (1 + \frac{V_{TAS}}{C_{f_2}}) \tag{31}$$

Where, C_{f_1} and C_{f_2} are the thrust specific fuel consumption coefficients specified in BADA tables.

3.4.3 Engine Thrust

To calculate the nominal fuel flow rate, it is necessary to calculate the engine thrust at different phase of flight. The BADA model provides coefficients that allow the calculation of the following thrust levels:

3.4.3.1 Maximum Climb and Take-off Thrust

The maximum climb thrust at standard atmosphere conditions, $(Thr_{\text{maxclimb}})\text{ISA}$, is calculated Newton's as a function of geo potential pressure altitude, H_p [ft]; true airspeed, V_{TAS} [kt]; and temperature deviation from standard atmosphere, ΔT [K]. Here only jet engine type was considered, The equation for maximum climb and take-off thrust as follows:

$$(Thr_{\text{maxclimb}})\text{ISA}=C_{T_{c,1}} \times (1-\frac{H_p}{C_{T_{c,2}}}+C_{T_{c,3}} \times H_p{}^2) \quad (32)$$

Where, $C_{T_{c,1}}$, $C_{T_{c,2}}$ and $C_{T_{c,3}}$ are climb thrust coefficient specified in the BADA tables.

The maximum climb thrust is corrected for temperature deviations from standard atmosphere, ΔT, in the following manner:

$$Thr_{\text{maxclimb}} = (Thr_{\text{maxclimb}})\text{ISA} \times (1 - C_{T_{c,5}} \times \Delta T_{eff}) \quad (33)$$

Where,

$$\Delta T_{eff} = \Delta T - C_{T_{c,4}} \quad (34)$$

With the limits,

$$0.0 \le C_{T_{c,5}} \times \Delta T_{eff} \le 0.4 \quad (35)$$

$$C_{T_{c,5}} \ge 0.0 \quad (36)$$

Where, $C_{T_{c,4}}$ and $C_{T_{c,5}}$ are thrust temperature coefficient specified in the BADA tables. This maximum climb thrust is used for both take-off and climb phases.

3.4.3.2 Maximum Cruise Thrust

The normal cruise thrust is by definition set equal to drag ($Thr = D$). However, the maximum amount of thrust available in cruise situation is limited. The maximum cruise thrust is calculated as a ratio of the maximum climb thrust as follows:

$$(Thr_{\text{cruise}})\text{MAX} = C_{T_{cr}} \times Thr_{\text{maxclimb}} \quad (37)$$

The Maximum cruise thrust coefficient $C_{T_{cr}}$ is currently uniformly set for all aircraft of value 0.95.

3.4.3.3 Descent Thrust

Descent thrust is calculated as a ratio of the maximum climb thrust, with different correction factors used for high and low altitudes, and approach and landing configurations, that is:

If $H_p > H_{p,des}$

$$Thr_{\text{des,high}} = C_{T_{\text{des,high}}} \times Thr_{\text{maxclimb}} \tag{38}$$

Where, $H_{p,des}$ is the transition altitude, $C_{T_{\text{des,high}}}$ is high altitude descent thrust coefficient specified in BADA tables.

If $H_p \le H_{p,des}$

Cruise configuration: $$Thr_{\text{des,low}} = C_{T_{\text{des,low}}} \times Thr_{\text{maxclimb}} \tag{39}$$

Where, $C_{T_{\text{des,low}}}$ is the low altitude descent thrust coefficient specified in BADA tables.

Approach configuration: $$Thr_{\text{des,app}} = C_{T_{\text{des,app}}} \times Thr_{\text{maxclimb}} \tag{40}$$

Where, $C_{T_{\text{des,app}}}$ is the approach thrust coefficient specified in BADA tables.

Landing Configuration: $$Thr_{\text{des,ld}} = C_{T_{\text{des,ld}}} \times Thr_{\text{maxclimb}} \tag{41}$$

Where, $C_{T_{\text{des,ld}}}$ is the landing thrust coefficient specified in BADA tables.

4. Simulation and Result

In this section the simulation and result of the fuel optimal trajectories are shown for three different length (short, medium and long haul) trajectories considering no wind. All the analysis of the simulation has been done using Matlab 2013[a]. The coordinates of the trajectory were chosen using skyvector website [15] .

4.1 Short Haul Flight

To analyze the short haul flight, the flight from Lisbon to Geneva was considered. The 4D waypoint network of this short haul flight consists of two trajectories, and has total 22 waypoints including the initial and final waypoints, and each trajectory has 12 waypoints including the initial and final waypoints. Airplane A1 (which is a short medium range twinjet narrow body airliner) was used to analyze the flight trajectories. (table 1 and 2) Show the waypoints lists for both of the trajectories. Each waypoint is defined in geodetic coordinates (λ , φ , h) and their associated distance Δd_k , travel time $d\tau_k$ and consumed fuel df_k between the waypoints are also shown.

Table 1: List of waypoints in 1st trajectory for short haul flight

waypoint	λ [deg]	φ [deg]	h [feet]	Δd_k [nm]	$d\tau_k$ [min]	df_k [kg]
Initial (P_1)	-9.0405	38.9955	3000	0	0	0
P_2	-8.9083	39.1087	10000	9.249827	2.371751	291.0612
P_3	-8.624	39.33417	20000	19.01912	3.437191	348.0156
P_4	-7.7987	39.8783	33000	50.39803	7.295251	535.3803
P_5	-6.9993	40.2513	39000	43.16538	5.748997	294.6361
P_6	-3.3707	43.227	39000	242.0397	32.48854	1176.085
P_7	0.1303	44.729	39000	176.7117	23.71969	858.6528
P_8	3.5963	44.9543	39000	148.8367	19.97808	723.2065
P_9	3.87217	45.1205	33000	15.45767	2.058735	7.823191
P_{10}	4.6985	45.41983	20000	39.46054	5.71202	32.05871
P_{11}	5.336	45.606	10000	29.19265	5.275779	42.20624
Final (P_{22})	5.7553	45.884	3000	24.30017	5.618537	54.83692
Total				797.8314	113.7046	4363.963

The trajectories were chosen such a way that the climb and descent phases of the first trajectory are smaller than the second trajectory but the cruise phase of the first trajectory is bigger than the second trajectory, therefore the total distance from the initial waypoint to final waypoint for both of the trajectories are more or less same. In order to find the fuel optimal trajectory from the 4D waypoint network possible connection between waypoints in both trajectories were established, and their associated distance Δd_k , travel time $d\tau_k$ and consumed fuel df_k between these possible waypoints connections were calculated.

Table 2: List of waypoints in 2nd trajectory for short haul flight.

waypoint	λ [deg]	φ [deg]	h [feet]	Δd_k [nm]	$d\tau_k$ [min]	df_k [kg]
Initial (P_1)	-9.0405	38.9955	3000	0	0	0
P_{12}	-8.835	39.0883	10000	11.16491	2.862798	351.3225
P_{13}	-8.49983	39.30183	20000	20.28586	3.66612	371.1947
P_{14}	-7.59217	39.7763	33000	50.94383	7.374258	541.1783
P_{15}	-6.715	40.11317	39000	45.32355	6.036433	309.3672
P_{16}	-1.765	41.631	39000	243.352	32.6647	1182.462
P_{17}	0.5565	43.9993	39000	175.4797	23.55432	852.6664
P_{18}	3.6277	44.85317	39000	141.8812	19.04446	689.4095
P_{19}	3.9993	44.9983	33000	18.13834	2.415762	9.179894
P_{20}	4.8617	45.261	20000	39.98448	5.787862	32.48437
P_{21}	5.4975	45.5203	10000	31.13026	5.625951	45.00761
Final (P_{22})	5.7553	45.884	3000	24.40439	5.642634	55.0721
Total				802.0885	114.6753	4439.345

The fuel optimal trajectory was generated from the 4D waypoint network using the Dijkstra's shortest path algorithm. The fuel optimal trajectory contains 9 waypoints [initial waypoint (P_1)→ P_2→ P_3→ P_4→ P_5→ P_{18}→ P_{19}→ P_{11}→ final waypoint (P_{22})], the distance between the initial and final waypoints in fuel optimal trajectory is 777.7 nm. The comparison of fuel consumed in different phases of flight for these two trajectories and fuel optimal trajectory are shown in (table 3).

Table 3: Fuel consumed from initial to final waypoint in different trajectories for short haul flight.

Trajectory	Fuel consumed [kg]			Total [kg]
	Climb	Cruise	Descent	
1	1469.1	2757.9	136.9	4363.9
2	1573.1	2724.5	141.7	4439.3
Fuel optimal	1469.1	2652.8	136.1	4258

As seen in (table 3), by using the fuel optimal trajectory for the short haul flight (Lisbon – Geneva) the aircraft consumes 105.9 kg of less fuel than the first trajectory, which is equivalent to 2.4% less fuel than the first trajectory and consumes 181.3 kg of less fuel than the second trajectory, which is equivalent to 4.1% less fuel than the second trajectory. The fuel optimal trajectory in 3D is shown in (figure 1).

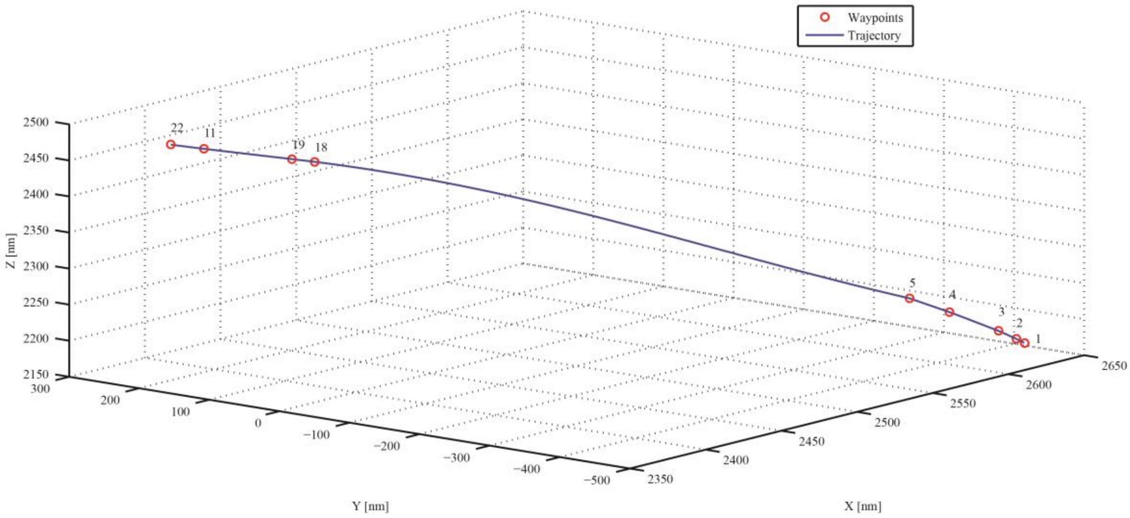

Figure 1: 3D fuel optimal trajectory in geocentric coordinates for short haul flight.

In (figure 1) the fuel optimal trajectory is represented by the blue line and the red circles around the trajectory are the waypoints.

4.2 Medium Haul Flight

To analyze the medium haul flight, the flight from Lisbon to Stockholm was considered. There are also two trajectories between the initial and final waypoints in the 4D waypoint network, each trajectories has 13 waypoints including the initial and final waypoints, and total 24 waypoints are there in the 4D waypoint network including the initial and final waypoint. Airplane A2 (which is a long range wide body twinjet airliner) was used to analyze the flight trajectories. (table 4 and 5) Show the waypoints lists for both of the trajectories.

Table 4: List of waypoints in 1st trajectory for the medium haul flight

waypoint	λ [deg]	φ [deg]	h [feet]	Δd_k [nm]	$d\tau_k$ [min]	df_k [kg]
Initial (P_1)	-9.0405	38.9955	3000	0	0	0
P_2	-8.9373	39.1525	10000	10.63985	2.665515	1070.631
P_3	-8.643	39.6385	24000	32.29915	5.529098	1724.94
P_4	-8.0007	40.5407	37000	61.77433	8.291856	1859.863
P_5	-7.7847	40.942	41000	26.05963	3.243938	589.0991

waypoint	λ [deg]	φ [deg]	h [feet]	Δd_k [nm]	$d\tau_k$ [min]	df_k [kg]
P_6	-4.752	46.1707	41000	340.8976	42.43539	5385.051
P_7	1.07817	49.6497	41000	314.9914	39.21055	4975.819
P_8	9.07617	53.515	41000	379.0242	47.18143	5987.324
P_9	14.4575	57.839	41000	318.0823	39.59531	5024.645
P_{10}	14.75417	58.0005	37000	13.62262	1.695762	31.54117
P_{11}	15.78983	58.624	24000	49.92285	6.807662	161.8522
P_{12}	17.0113	59.2063	10000	51.77227	9.043191	287.5735
Final (P_{24})	17.73983	59.3445	3000	23.95284	5.538229	212.0034
Total				1623.039	211.2379	27310.34

Table 5: List of waypoints in 2nd trajectory for the medium haul flight

waypoint	λ [deg]	φ [deg]	h [feet]	Δd_k [nm]	$d\tau_k$ [min]	df_k [kg]
Initial (P_1)	-9.0405	38.9955	3000	0	0	0
P_{13}	-8.8405	39.1047	10000	11.47263	2.874146	1154.43
P_{14}	-8.455	39.576	24000	33.57806	5.748028	1793.241
P_{15}	-7.808	40.4545	37000	60.65319	8.141368	1826.109
P_{16}	-7.413	40.8377	41000	29.26358	3.642769	661.5269
P_{17}	-0.2773	44.76	41000	393.6387	49.00066	6218.184
P_{18}	4.6187	50.023	41000	374.0856	46.56667	5909.311
P_{19}	10.92483	54.85883	41000	371.7582	46.27695	5872.545
P_{20}	15.0405	57.2845	41000	201.3458	25.06379	3180.595
P_{21}	15.39	57.4757	37000	16.19891	2.016462	37.50619
P_{22}	16.496	58.17	24000	54.91818	7.488843	178.0473
P_{23}	17.504	58.94117	10000	56.26139	9.827318	312.5087
Final (P_{24})	17.73983	59.3445	3000	25.36559	5.864875	224.5074
Total				1628.54	212.5119	27368.51

The fuel optimal trajectory contains 9 waypoints [initial waypoint (P_1)→ P_2→ P_3→ P_4→ P_5→ P_{20}→ P_{21}→ P_{23}→ final waypoint (P_{24})], which was generated implying Dijkstra's algorithm, the distance between the initial and final waypoints in fuel optimal trajectory for this flight is 1596.5 nm.

Table 6: Fuel consumed from initial to final waypoint in different trajectories for medium haul flight

Trajectory	Fuel consumed [kg]			Total [kg]
	Climb	Cruise	Descent	
1	5244.5	21372.8	692.97	27310.3
2	5435.3	21180.6	752.6	27368.5
Fuel optimal	5244.5	20744.4	742.2	26731.1

The comparison of consumed fuel in different phases of flight for different trajectories including the fuel optimal trajectory are shown in (table 6).

From the initial waypoint to reach the final waypoint using the fuel optimal trajectory the aircraft consumes 579.2 kg of less fuel than the first trajectory and consumes 637.4 kg of less fuel than the second trajectory. In other word by using the fuel optimal trajectory for the medium haul flight (Lisbon – Stockholm) the aircraft consumes 2.1% less fuel than the first trajectory, and 2.3% less fuel than the second trajectory. The fuel optimal trajectory in three dimension is shown in (figure 2).

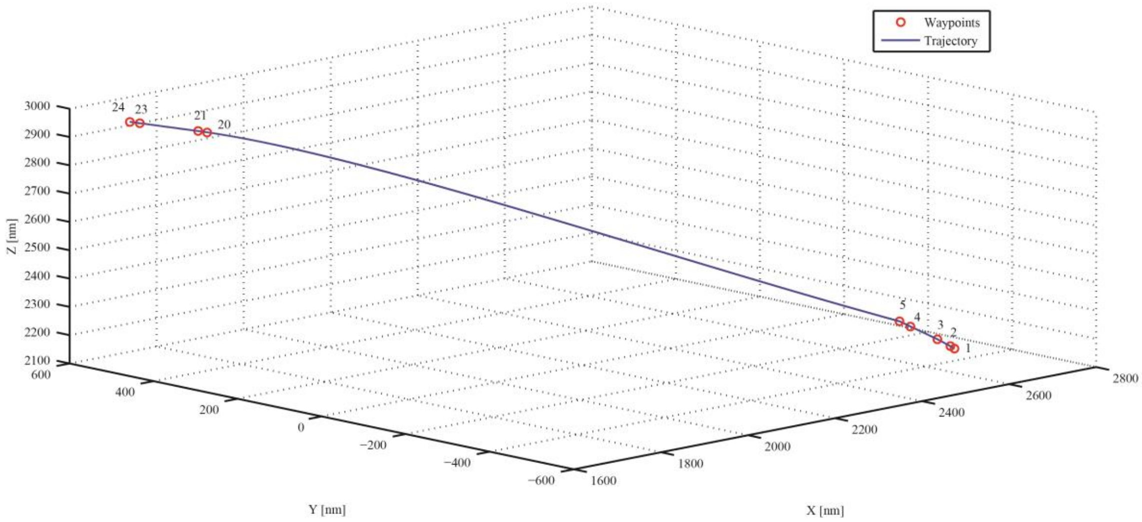

Figure 2: 3D fuel optimal trajectory in geocentric coordinates for medium haul flight.

The blue curve in (figure 2) corresponds to the fuel optimal trajectory for the medium haul flight (Lisbon – Stockholm) and the red circles around the curve are the waypoints of the fuel optimal trajectory.

4.3 Long Haul Flight

The flight from Lisbon to Montreal was considered to analyze the long haul flight. The 4D waypoint network of the long haul flight also consists of two trajectories between the initial and final waypoints, each trajectories has 14 waypoints including the initial and final waypoints, and total 26 waypoints are in the whole 4D waypoint network including initial and final waypoints. Airplane A2 (which is a long range wide body twinjet airliner) was used to analyze the flight trajectories. The waypoints lists of both trajectories are shown in (table 7 and 8).

Table 7: List of waypoints in 1st trajectory of long haul flight

waypoint	λ [deg]	φ [deg]	h [feet]	Δd_k [nm]	$d\tau_k$ [min]	df_k [kg]
Initial (P_1)	-9.0405	38.9955	3000	0	0	0
P_2	-9.22083	39.1	10000	10.5683	2.64759	1063.431
P_3	-9.8425	39.3857	24000	33.76592	5.780186	1803.274
P_4	-10.9352	39.9543	37000	61.15747	8.209056	1841.291
P_5	-11.74	40.32817	43000	43.3812	5.40015	959.6066
P_6	-22.5022	43.5023	43000	518.4016	64.53132	8227.743
P_7	-35.132	44.73617	43000	550.8432	68.56969	8742.636
P_8	-44.9847	47.4295	43000	442.3112	55.05948	7020.084
P_9	-58.667	48.5647	43000	555.3268	69.12781	8813.796
P_{10}	-70.3565	46.4947	43000	491.3069	61.15854	7797.714
P_{11}	-70.809	46.4135	37000	19.45513	2.421801	43.59241
P_{12}	-71.9328	46.21	24000	48.42787	6.6038	157.0053
P_{13}	-73.0908	45.9335	10000	51.23244	8.948898	284.575
Final (P_{26})	-73.6412	45.7947	3000	24.56775	5.680405	217.4459
Total				2850.746	364.1387	46972.19

Table 8: List of waypoints in 2nd trajectory of long haul flight

waypoint	λ [deg]	φ [deg]	h [feet]	Δd_k [nm]	$d\tau_k$ [min]	df_k [kg]
Initial (P_1)	-9.0405	38.9955	3000	0	0	0
P_{14}	-9.2387	39.05683	10000	10.03791	2.514717	1010.061
P_{15}	-9.94583	39.2603	24000	35.28932	6.040968	1884.631
P_{16}	-11.2588	39.4515	37000	62.29715	8.362034	1875.604
P_{17}	-11.9673	39.9493	43000	44.44929	5.533107	983.2331
P_{18}	-24.8818	42.095	43000	600.2876	74.7246	9527.386
P_{19}	-34.374	43.996	43000	433.2285	53.92886	6875.93
P_{20}	-44.3497	46.44083	43000	448.0273	55.77103	7110.806
P_{21}	-61.77	47.44	43000	717.2308	89.28184	11383.43
P_{22}	-70.163	46.2543	43000	353.4368	43.99628	5609.525
P_{23}	-70.557	46.102	37000	18.61899	2.317716	41.71889
P_{24}	-71.739	45.9043	24000	51.21564	6.98395	166.0434
P_{25}	-72.9952	45.81	10000	53.07175	9.270174	294.7915
Final (P_{26})	-73.6412	45.7947	3000	27.16449	6.280807	240.4293
Total				2854.355	365.0061	47003.6

Possible connection between waypoints in both trajectories were established, and their associated distance Δd_k , travel time $d\tau_k$ and consumed fuel df_k between these possible waypoints connections were calculated in order to find the fuel optimal trajectory by implying Dijkstra's shortest path algorithm.

The fuel optimal trajectory of the flight between Lisbon to Montreal contains 9 waypoints [initial waypoint (P_1)→ P_{14}→ P_3→ P_4→ P_5→ P_{22}→ P_{11}→ P_{13}→ final waypoint (P_{26})], the distance between the initial and final waypoints in fuel optimal trajectory is 2777 nm. The comparison of fuel consumed in different phases of flight for different trajectories and the fuel optimal trajectory are shown in (table 9).

Table 9: Fuel consumed from initial to final waypoint in different trajectories for long haul flight

Trajectory	Fuel consumed [kg]			Total [kg]
	Climb	Cruise	Descent	
1	5667.6	40601.9	702.6	46972.2
2	5753.5	40507.1	742.98	47003.6
Fuel optimal	5652.1	39284.9	712.5	45649.5

Using the fuel optimal trajectory in long haul flight the aircraft consumed 1322.7 kg of less fuel than the first trajectory and consumed 1354.1 kg less fuel than the second trajectory. So in the fuel optimal trajectory for the long haul flight the aircraft consumes 2.8% less fuel than the first trajectory, and 2.9% less fuel than the second trajectory. The 3D fuel optimal trajectory is shown in (figure 3).

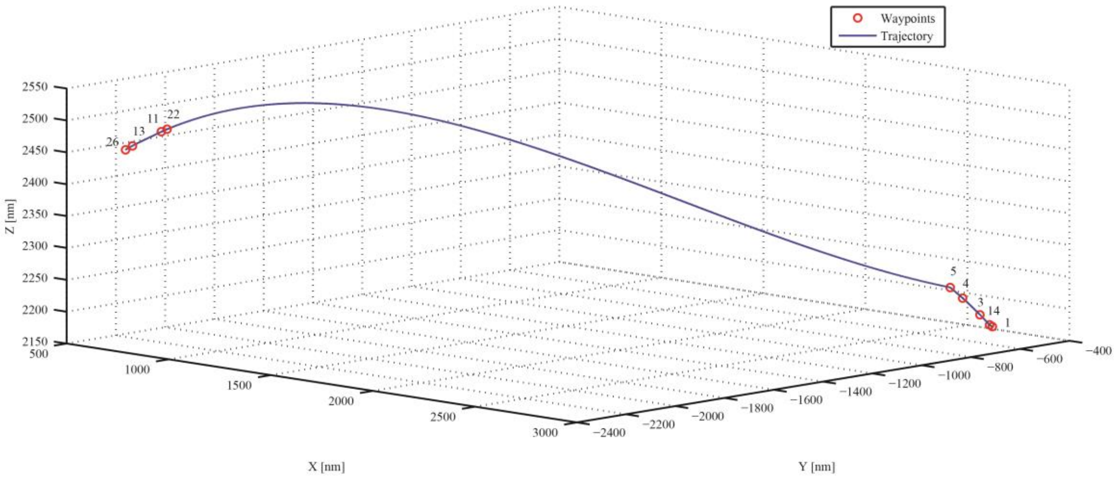

Figure 3: 3D fuel optimal trajectory in geocentric coordinates for long haul flight.

The blue curve in (figure 3) is the fuel optimal trajectory and the red circles around it are the waypoints of that trajectory. In this long haul flight the cruise phase is really large compare to its climb and descent phases, therefore the waypoints in the climb and descent phases are seems really close to each other in the figure.

5. Conclusion

This study is based on finding the fuel optimal trajectories of climb, cruise and descent phases of the flight, without the takeoff and landing phases of the flight. In this work several steps were made in order to achieve a complete trajectory from a 4D waypoint networks that optimize the fuel consumption. This study uses Dijkstra's shortest path algorithm that find an fuel optimal trajectory from a given 4D waypoint networks, this technique was used to compare different length (short, medium and long haul) flights.

The analysis results show promising potential for reduction of consumed fuel in different flights via using the Dijkstra's shortest path algorithm, across a range of common aircrafts and routes. The results suggest that by flying fuel optimal trajectory for short haul flight, it is possible to save 2.4−4.1% on fuel burn, which is equivalent to 105.9 – 181.3 kilograms of fuel for Airplane A1. In medium haul flight by flying the fuel optimal trajectory can potentially save 2.1−2.3% fuel, reducing fuel burn by 579.2 – 637.4 kilograms for Airplane A2. For long haul flight it is possible to save 2.8−2.9% on fuel burn, which is equivalent to 1322.7 – 1354.1 kilogram of fuel for Airplane A2. In general the savings of the fuel is proportional to the trip lengths, and depends on the aircraft types.

6. References

[1] ICAO, "ICAO Environmental Report: Aviation and Climate change," *ICAO*, 2013.

[2] B. Robenson, "Fuel Conservation Strategies: Cost Index Explained," *Boeing*, 2007, pp.26-28.

[3] W. Roberson and J. A. Johns, "Fuel Conservation strategies: Takeoff and Climb," *Boeing*, 2008, pp. 25-28.

[4] W. Roberson and J. A. Johns, "Fuel Conservation Strategies: Descent and Approach," *Boeing*, 2008, pp. 25-28.

[5] Hagelauer, P. and Mora-Camino, F., "Evaluation of Practical Solutions for Onboard Aircraft Four-Dimensional Guidance," *Journal of Guidance, Control, and Dynamics*, Vol. 20, No. 5, 1997, pp. 1052 - 1054.

[6] Bryson, A. E. and Y. C. Ho, "*Applied Optimal Control: Optimization, Estimation and, Control*", Taylor & Francis, New York, 1975, Ch. 2, pp. 42-89.

[7] Calise, A. J. "Extended Energy Management for Flight Performance Optimization, *AIAA Journal*, VOl. 15, No. 3, March 1977, pp. 314-321.

[8] Calise A. J. and D. D. Moerder, "Singular Perturbation Techniques for Real Time Aircraft Trajectory Optimization and Control", *NASA CR-3597*, 1982.

[9] Cormen T. H., Leiserson C. E., Rivest R. L., and Stein C., "*Introduction to Algorithms*", London, England: The MIT Press, 2009 3rd ed, pp. 658-664.

[10] Hart C., "Graph Theory Topics in Computer Networking", 2013, pp. 13-20.

[11] Dasgupta S., Papadimitriou C. H. and Vazirani U. V.," *Algorithms*", McGraw-Hill, New York, July 18, 2006, pp. 112-118.

[12] Seemkooei A. A., "Comparison of different algorithm to transform geocentric to geodetic coordinates," *Survey Review 36, 286* October 2002. pp. 627-632.

[13] "Aircraft Performance Summary Tables for the Base of Aircraft Data (BADA)," *Eurocontrol Experimental Centre*, Revision 3.4, June 2002.

[14] "User Manual for the Base of Aircraft Data (BADA)," *Eurocontrol Experimental Centre*, Revision 3.9, April 2011.

[15] "SkyVector," [Online]. Available: https://skyvector.com/. [Accessed October 2015].

Annex B – Article